RSC Advances

PAPER

View Article Online
View Journal | View Issue

Check for updates

Cite this: *RSC Adv.*, 2026, **16**, 9870

Mechanistic evaluation of static and dynamic adsorption of *Brassica juncea* derived gemini surfactants: implications to enhanced oil recovery

Lavisha Jangid, Keka Ojha and Ajay Mandal *

The adsorption of surfactants onto reservoir rock surfaces significantly affects the efficiency of enhanced oil recovery (EOR), as high retention reduces the effective concentration of surfactants during flooding. In the present study, the adsorption behaviour of synthesized Gemini surfactants (GS) on sandstone and carbonate rocks was evaluated using UV-vis spectroscopy under static and dynamic conditions. Equilibrium isotherm and kinetic models were applied to interpret the adsorption trends and assess the governing adsorption pathways. FESEM-EDX was employed to assess surface morphology and elemental mapping, while zeta potential measurements indicated charge modification. The static adsorption results showed that surfactant retention systematically decreased with increasing spacer length, indicating reduced packing efficiency for longer spacer Gemini structures. Dynamic adsorption shows very low surfactant retention, with maximum adsorption capacities of 0.013 mg g^{-1} for sandstone and 0.0087 mg g^{-1} for carbonate using Hexamine GS. Excessive surfactant adsorption during flooding causes chemical loss, but controlled surface adsorption is necessary for wettability alteration, as it facilitates a shift from oil-wet to water-wet conditions, thereby enhancing oil recovery. In this study, wettability alteration was investigated by measuring contact angles. Hexamine GS reduced contact angles by approximately 81% within a few minutes, accompanied by an efficient transition from an oil-wet to a water-wet state. Overall, the findings provide model-supported insight into spacer-length-dependent adsorption behaviour and highlight the potential of these bio-derived Gemini surfactants to minimise surfactant loss and improve wettability control in chemical EOR applications.

Received 24th January 2026
Accepted 12th February 2026

DOI: 10.1039/d6ra00648e

rsc.li/rsc-advances

Open Access Article. Published on 18 February 2026. Downloaded on 6/19/2026 8:10:42 PM.
This article is licensed under a Creative Commons Attribution-NonCommercial 3.0 Unported Licence.

1. Introduction

Chemical flooding, involving the injection of surfactants, polymers, and alkalis, has been extensively employed as an effective enhanced oil recovery (EOR) technique in both sandstone and carbonate reservoirs.[1,2] Among these methods, surfactant flooding has received significant attention due to its ability to improve microscopic displacement efficiency. The principal mechanisms include reduction of interfacial tension (IFT) to ultra-low values, which mobilizes residual oil; alteration of reservoir rock wettability from oil-wet to water-wet, which enhances fluid flow; and emulsification of trapped oil, which improves mobilization and sweep efficiency. Collectively, these effects contribute to substantial additional oil recovery beyond conventional methods.[3,4] Alkalis react with the acidic components of crude oil to generate *in situ* surfactants, which subsequently act through mechanisms similar to those of externally injected surfactants, though often with comparatively lower efficiency.[5] Polymers, on the other hand, enhance the viscosity of the injected water, thereby improving the mobility ratio between displacing and displaced fluids. This improvement in mobility control increases macroscopic sweep efficiency, ultimately contributing to higher oil recovery. The capillary number ($\mu v/\delta$), expressed as the ratio of viscous to interfacial forces, is widely recognized as a critical parameter governing the oil recovery factor. A higher capillary number corresponds to enhanced displacement efficiency and, consequently, greater oil recovery.[6,7] In practice, however, increasing the viscosity of the injected water or raising its flow rate to achieve higher capillary numbers is often constrained by injectivity issues and the risk of formation damage.[2,8] The interfacial tension (IFT) between crude oil and formation water typically ranges from 25 to 30 mN m^{-1}. Through the application of appropriate surfactants, the IFT can be reduced to ultra-low values, often below 10^{-3} mN m^{-1}, resulting in nearly a fourfold increase in the capillary number and substantial improvement in oil recovery.[9]

The major challenges associated with surfactant flooding are the high cost of surfactant formulations and the significant loss due to adsorption onto reservoir rock surfaces, which are strongly influenced by the surfactant's chemical nature and the rock's mineralogical composition.[10,11] The adsorption of surfactants onto reservoir rocks is governed by several

Enhanced Oil Recovery & Carbon Utilization and Storage Lab, Department of Petroleum Engineering, Indian Institute of Technology (Indian School of Mines), Dhanbad 826004, India. E-mail: ajay@iitism.ac.in

© 2026 The Author(s). Published by the Royal Society of Chemistry

Open Access Article. Published on 18 February 2026. Downloaded on 6/19/2026 8:10:42 PM.
This article is licensed under a Creative Commons Attribution-NonCommercial 3.0 Unported Licence.

mechanisms that depend on both the surfactant type and the rock surface characteristics. Electrostatic attraction is the most significant pathway: cationic surfactants bind to negatively charged sandstone or clay minerals, while anionic surfactants preferentially adsorb onto positively charged carbonate surfaces. When electrostatic interactions are weak or absent, van der Waals forces contribute to adsorption, although these interactions are relatively weak and highly distance-dependent.[12,13] In addition, mechanisms such as hydrogen bonding, polarization, ion exchange, ion pairing, hydrophobic bonding, and dispersion forces also play important roles. The combined influence of these interactions ultimately determines the extent of surfactant retention and the efficiency of chemical flooding processes. The loss of surfactants through interactions with reservoir rocks and fluids is one of the most critical factors governing the overall efficiency of a micellar flooding process[14,15]

The adsorption behaviour of surfactants in reservoirs is strongly influenced by operational and environmental parameters such as pH, temperature, ionic strength, and electrolyte concentration.[12,16,17] Even small changes in these factors can cause substantial variations in adsorption, leading to significant differences in surfactant efficiency during chemical flooding. The charge characteristics of the reservoir rock play a critical role in determining surfactant compatibility. In sandstone reservoirs, which generally possess negatively charged surfaces, anionic surfactants are favoured over nonionic and cationic counterparts because they exhibit lower adsorption and better stability under reservoir conditions. In contrast, carbonate reservoirs typically present positively charged surfaces, making cationic surfactants more suitable for reducing retention losses and improving recovery performance. Hence, careful matching of surfactant type with reservoir mineralogy, along with consideration of prevailing reservoir conditions, is essential to minimize adsorption losses and optimize the overall success of enhanced oil recovery processes. Studies on well-characterized adsorbents have provided insights into the structure of the adsorbed layer, adsorption mechanisms, and adsorption kinetics.[18–20] However, in heterogeneous systems such as carbonate rocks and soils, variations in mineralogy and surface chemistry make it difficult to predict the extent and dynamics of adsorption.[21] Moreover, environmental factors such as ionic strength, salinity, and pH further complicate the process, and a clear quantitative understanding of mineral-specific effects is still lacking.

In aqueous media, solid surfaces acquire positive or negative charges either through ionization/dissociation of surface groups or adsorption of ions from the surrounding solution.[22] The adsorption of surfactants onto these charged surfaces is strongly influenced by the electrical double layer, first proposed by Helmholtz in 1879 and later modified by Stern in 1924.[23,24] At low surfactant concentrations, surfactant molecules adsorb as monomers, forming a thin monolayer on rock surfaces or sediment surfaces. As concentration increases, adsorbed monomers aggregate into surface micellar structures, such as ad-micelles or hemimicelles.[25] It is essential that, after adsorption onto the rock surface, the remaining bulk surfactant concentration does not fall below the CMC, so that sufficient monomer availability and interfacial activity are maintained for effective wettability alteration and EOR performance.[26,27] It was discovered that surfactant adsorption had dual roles in chemical EOR. Excessive and irreversible adsorption was generally unfavourable because it caused surfactant loss and reduced the effective concentration available for interfacial tension reduction during flooding. However, a controlled, limited degree of surface adsorption was still necessary to achieve sufficient surface coverage for altering wettability by lowering the solid–oil interfacial free energy. Therefore, an optimal adsorption regime that minimised irreversible retention while enabling favourable surface modification was considered essential for effective surfactant flooding performance.[15,28,29]

Another important aim of using surfactants in reservoirs is to achieve wettability reversal, thereby increasing oil displacement and improving oil recovery. The wettability alteration is basically the surfactant adsorption in place of oil toward the rock surface by modifying surface energy and interaction with fluids. Some researchers,[30–35] highlighted that if there is some adsorption, the surfactant shows a strong interaction with the rock surface, which can transform an oil-wet surface into a more water-wet condition. This shift enhances water imbibition, reduces capillary forces restraining oil, and promotes the release of trapped hydrocarbons. A surfactant–rock interaction not only improved microscopic displacement efficiency, which directly affects wettability alteration, but also enhanced oil recovery by complementing IFT reduction.

The adsorption of surfactants onto porous media has traditionally been studied using equilibrium isotherm models. These isotherms describe the surfactant's equilibrium adsorption capacity on the solid surface as a function of its equilibrium concentration in solution at a given temperature, allowing an estimate of the validity of surfactant application.[36,37] Therefore, the interpretation of surfactant adsorption isotherms has been a central focus of surface and colloid chemists for many years. There are many modelling techniques used to understand the adsorption mechanism and adsorbed layer type, such as Linear, Langmuir, Freundlich, Temkin, BET, Redlich–Peterson, and Hill, based on the complexity of the adsorption process.[38] Langmuir's model implies that monolayer adsorption occurs on a homogeneous surface, whereas Freundlich's model accounts for multilayer adsorption on heterogeneous surfaces.[39,40] Alongside kinetic models including pseudo-first order, pseudo-second order, and intra-particle diffusion approaches.[41,42] Kinetic models are mainly useful in describing the rate at which solute molecules are transferred from the bulk solution to the solid–liquid (surfactant) interface and the residence time of adsorbates on the surface. The adsorption rate is governed by the number of molecules adsorbing on the adsorbent surface per unit time and the number of molecules colliding per unit time.[38]

Despite significant progress in understanding adsorption mechanisms and modelling approaches, most existing studies have focused on conventional single-chain or synthetic surfactants. In contrast, systematic investigations of bio-derived Gemini surfactants remain scarce, particularly under

Open Access Article. Published on 18 February 2026. Downloaded on 6/19/2026 8:10:42 PM.
This article is licensed under a Creative Commons Attribution-NonCommercial 3.0 Unported Licence.

reservoir-relevant static and dynamic conditions. Considering their structural advantages, such as low CMC, ability to achieve ultralow IFT, and reduced adsorption losses, Gemini surfactants synthesized from renewable feedstocks hold strong potential for sustainable chemical EOR.[43,44] However, the adsorption behaviour of these surfactants differs from that of conventional surfactants in sandstone and carbonate systems, and their easy availability impacts the economy.[11] Thus, in sandstone reservoirs, adsorption behaviour is mainly dominated by quartz and silicates, *via* hydrogen bonding, van der Waals interactions, and weak electrostatic forces, whereas in carbonate systems dominated by calcite, electrostatic attraction and ion exchange play dominant roles.[45] While a few studies have explored adsorption phenomena in both rock surfaces, few have combined static and dynamic adsorption experiments with mechanistic modelling to capture both equilibrium behaviour and flow-controlled retention, particularly for naturally derived Gemini surfactants. The advancement of Gemini surfactants has gained importance for sustainability in chemical EOR. The search for eco-friendly, bio-derived surfactants stems from both environmental concerns and the rising costs associated with petrochemical-based surfactants. Vegetable oils such as soybean, sunflower, and mustard oil are abundant, renewable sources of fatty acids and have been widely utilised in green chemistry approaches to synthesise biodegradable surfactants. Recent studies have shown that plant-derived surfactants can exhibit excellent interfacial properties, comparable to or even superior to those of conventional petrochemical-based surfactants, while offering improved biodegradability and reduced toxicity.[46–48] Despite this promise, systematic studies on the adsorption behaviour of naturally derived Gemini surfactants on reservoir rocks remain scarce. Most existing research has focused on synthetic Gemini surfactants, leaving a significant knowledge gap regarding the performance of bio-based alternatives under reservoir conditions.[49,50] Addressing this gap is crucial to evaluating the feasibility of naturally derived Gemini surfactants as cost-effective and environmentally friendly alternatives for enhanced oil recovery.

The present study seeks to bridge these gaps by systematically investigating the adsorption behaviour of mustard oil (*Brassica juncea*) derived Gemini surfactants onto sandstone and carbonate rocks under both static and dynamic conditions. By varying the spacer length from diamine to hexamine, the influence of molecular architecture on adsorption is comprehensively evaluated. Surfactant retention was quantified using UV-vis spectroscopy, and adsorption mechanisms were analysed *via* multiple static adsorption isotherms, including Linear, Langmuir, Freundlich, and Hill isotherms, along with kinetic models such as pseudo-first order, pseudo-second order, and intra-particle diffusion to capture equilibrium and rate-controlling processes. Analysis, including FESEM-EDX for surface morphology and elemental mapping, zeta potential measurements for surface charge modification, and contact-angle measurements for wettability alteration, was employed to provide a holistic understanding of rock–fluid interactions. The adsorption study shows that adsorption reduces with increasing spacer length. The increase in spacer length also induces a rapid, effective alteration in wettability. The dynamic adsorption study was analyzed for systematic determination of the potential of Gemini surfactants in real field applications. The results confirm that mustard oil-derived Gemini surfactants combine the advantages of low adsorption and strong wetting modification with the added benefit of sustainability and environmental benignity. By linking spacer length, adsorption behaviour, and wettability alteration, this work advances the mechanistic understanding of bio-derived Gemini surfactants and highlights their potential as cost-effective, eco-friendly alternatives for EOR in sandstone and carbonate reservoirs.

2. Materials and methods

2.1. Materials and analytical characterization

In this study, the Gemini surfactants used have been synthesised in our previous work,[46] which was derived from mustard oil. The sandstone and carbonate cores were utilized in this study to assess the impact of our non-ionic Gemini surfactants on both rock types through wettability and core-flooding studies. The diameter of the cores was about 1.5 inches, and the length was 8 inches. The X-ray diffraction of both sandstone and carbonate rock samples for mineralogical analysis was performed using a Malvern Analytical Aeris X-ray diffractometer. XRD analysis of the sandstone samples reveals 99% of quartz (Qz) as the predominant mineral, while the carbonate rock samples primarily consist of calcite ($CaCO_3$) as shown in Fig. S1 in the SI. Elemental analysis of both rock samples was performed using a wavelength-dispersive X-ray fluorescence spectrometer (Rigaku Primus IV). The XRF of the sandstone sample shows a high 88.1% SiO_2 mass percentage, indicating a predominant quartz composition, whereas in the carbonate sample, CaO was present at a maximum of 93%, indicating calcium carbonate minerals, as shown in Table S1 in the SI. Detailed mineralogical and elemental analyses are provided in the SI, Sections S.1 and S.2.

2.2. Synthesis of gemini surfactants and characterization

A two-step reaction scheme was carried out in the synthesis of the Gemini surfactants. In the first step, mustard oil was *trans*-esterified with methanol (CH_3OH) to produce mustard oil fatty methyl esters (MFMEs). These MFMEs were then converted into the corresponding Gemini surfactants through direct aminolysis using four different amine spacers, including *N*,*N*-diethylenetriamine, *N*,*N*-triethylenetetramine, *N*,*N*-

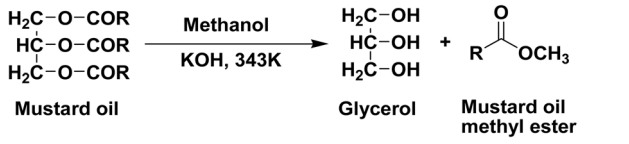

Fig. 1 First step reaction pathway of *trans*-esterification using mustard oil.

© 2026 The Author(s). Published by the Royal Society of Chemistry

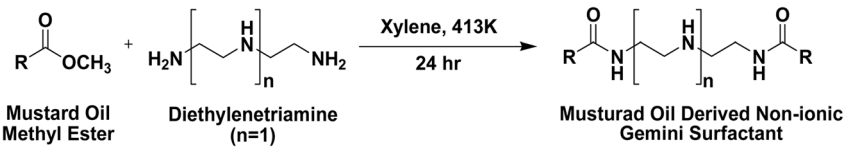

Fig. 2 The reaction scheme for Triamine GS synthesis, illustrated in the above figure, where $n = 1$, for the spacer diethylenetriamine. The same scheme was applied to the synthesis of tetramine GS, pentamine GS, and hexamine GS, with $n = 2$, 3, and 4, respectively.

Open Access Article. Published on 18 February 2026. Downloaded on 6/19/2026 8:10:42 PM. This article is licensed under a Creative Commons Attribution-NonCommercial 3.0 Unported Licence.

tetraethylenepentamine, and *N*,*N*-pentaethylenehexamine. The reaction scheme for transesterification, as represented in Fig. 1, and the surfactant synthesis using direct aminolysis, as represented in Fig. 2. These surfactants are classified as non-ionic because their hydrophilicity arises from electrically neutral amide and amine groups capable of shydrogen bonding, with no permanently charged head groups present and only pH-dependent, reversible protonation of amines. Confirmation of the chemical structure of the synthesized Gemini surfactant was determined using FTIR and NMR analysis. The FTIR peak shift from the ester group at 1743 cm^{-1} to 1657, 1652, 1655, 1659 cm^{-1} for the increasing spacer length of synthesized surfactants confirms the amide group of spacers. The NMR chemical shift (δ) values of 0.84–0.85 (singlet) and 1.22–1.24 (singlet) confirm the presence of terminal methyl ($-CH_3$) and methylene ($-CH_2-$) groups with unsaturation ($H_2C = CH-CH_2$) in the long fatty acid chains as a singlet at 1.88–2.01 ppm(δ) and the synthesized surfactant molecule is indicated by the presence of a doublet at chemical shift (δ) values of 2.47–2.77 ppm. A detailed description of the synthesis and characterization has been reported earlier in our previous work.[46]

2.3. Static adsorption study

Static adsorption experiments were performed to examine the interaction between the synthesized Gemini surfactants and sandstone and carbonate rock. It is essential that, after adsorption onto the rock surface, the remaining bulk surfactant concentration does not fall below the CMC, so that sufficient monomer availability and interfacial activity are maintained for effective wettability alteration and EOR performance. To acknowledge that both rock samples were finely ground and saturated with 100 ppm of synthesized Gemini surfactants. Surfactants with the same bulk concentration of 100 ppm but different spacer lengths were tested to assess the effects of molecular structure and spacer length on rock–fluid interactions. The mixtures were agitated on a Tarsons Rotospin at 50 rpm over time intervals up to 7 days to ensure sufficient contact for saturation after the addition of the fine rock powders and to achieve equilibrium conditions. The agitated samples were then centrifuged at 3000 rpm for 30 minutes to separate the solid and liquid phases. The upper layer of the surfactant solution, after separation, was analysed by UV spectroscopy. UV-vis analysis is based on the absorption of monochromatic light by chemical species, where each compound exhibits a distinct absorbance peak at a characteristic wavelength. To quantify the remaining surfactant concentration in the supernatant, a calibration curve was prepared using standard surfactant solutions. The amount of surfactant adsorbed at equilibrium was calculated using eqn (1), based on the initial surfactant concentration used (C_i) and final equilibrium surfactant concentration after the adsorption (C_e), the volume of the surfactant solution (V) in litres and the mass of the adsorbent rock in grams.

$$q_{e(static)} = \frac{V(C_i - C_e)}{m} \quad (1)$$

2.4. Surface morphology study (FESEM)

The surface morphology of the rock samples before and after surfactant treatment was examined using Field Emission Scanning Electron Microscopy (FESEM). Samples were sputter-coated with a thin layer of gold to ensure conductivity, and imaging was performed at various magnifications (5000–50 000×) using an FEI Quanta 200 FEG microscope under high vacuum.

2.5. Surface charge measurements

To determine the surface charge of the untreated and treated rock samples, zeta potential measurements were carried out using an AntonPaar Litesizer 500. The crushed rock particles were dispersed in surfactant samples, and their zeta potentials were measured at different time points to assess electrostatic interactions influencing surfactant adsorption.

2.6. Static adsorption isotherm modelling

A quantitative assessment of surfactant loss due to adsorption onto the reservoir rock during surfactant flooding-based EOR is crucial, as it enables fitting experimental data to established models. This connection between laboratory measurements and practical design and economic considerations is important. The isotherm models, including the linear, Langmuir, Freundlich, Redlich–Peterson, and Hill Isotherm models, are very useful for predicting surfactant loss during enhanced oil recovery by surfactant flooding across different reservoir simulation tools. By comparing the degree of fit obtained by different adsorption models, one can interpret the characteristic behaviour of the adsorption, whether it is monolayer or multilayer, homogeneous or heterogeneous, and physical or chemical. A detailed description of these models is provided in the SI, Section S.3.

2.7. Adsorption kinetics

Kinetic modelling was employed to elucidate the underlying adsorption mechanism and to identify the potential rate-

Open Access Article. Published on 18 February 2026. Downloaded on 6/19/2026 8:10:42 PM. This article is licensed under a Creative Commons Attribution-NonCommercial 3.0 Unported Licence.

controlling steps governing the process. The experimental kinetic data were evaluated using three commonly applied models: the pseudo-first-order, pseudo-second-order, and intraparticle diffusion models. These models play a critical role in determining the efficiency of the sorption process. The pseudo-first order model describes physisorption with initial adsorption stages, while the pseudo-second order model highlights the interaction between adsorbate and adsorbent.[51] The intraparticle diffusion model by Weber and Morris describes the diffusion on the pore scale, taking into account the boundary layer effect of diffusion.[52] The detailed description of these models is provided in the SI, Section S.4.

2.8. Thermodynamic analysis

The Gibbs energy change (ΔG°) specifies the spontaneity degree of an adsorption process, with more negative values indicating a more energetically favourable process. According to the thermodynamic law, ΔG° of adsorption can be calculated from eqn (2):

$$\Delta G = -RT\ln K^0 \quad (2)$$

where K^0 is dimensionless, R is the universal thermodynamic constant with 8.314 J mol^{-1} K^{-1}, and T is the absolute temperature in Kelvin.

Langmuir equilibrium constant K_L (L mg^{-1}) used to calculate the K^0 of the adsorption reaction, as shown in the above equation K^0 is a dimensionless standard equilibrium constant that needs to be calculated to calculate the ΔG using the following eqn (3):

$$K^0 = \frac{K_L \times M \times 1000}{C^0} \quad (3)$$

where M is the molar mass of the adsorbate (surfactant) (gm mol^{-1}), the factor 1000 for converting mg to gm, and C^0 is the standard state concentration (1 mol L^{-1}) according to IUPAC.

$$K^0 = K_L \times M \times 1000 \quad (4)$$

Now, ΔG should be calculated using K^0 which was obtained by the above eqn (4).[53]

2.9. Dynamic adsorption and desorption study

Dynamic adsorption tests were performed on sandstone and carbonate core samples using core flooding experiments, as shown in Fig. 3. Both experiments were conducted under a confining pressure of 1000 psi and a liquid injection rate of 0.333 mL min^{-1}. The effluent from the core flood was analysed using a UV-vis spectrometer.[54,55] Dynamic adsorption was calculated using the following eqn (5):

$$q_{e(dynamic)} = \frac{C_0 V - \sum_{i=1}^{N} C_i V_i}{m} \quad (5)$$

where $q_{e(dynamic)}$ (mg g^{-1} rock) is the surfactant's maximum capacity for dynamic adsorption, C_0 (ppm) denotes the injected gemini surfactant's concentration, V (L) denotes the total volume of the injected Gemini surfactant solution, C_i(ppm) shows the surfactant concentration at a specific effluent volume, and V_i (L) denotes the volume of the effluent collected at different time intervals, m (gm), denotes the total mass of the dry core sample, and N represents the total number of collected effluent samples.

Kwok *et al.* (1995) investigated the dynamic adsorption of an anionic surfactant on Berea sandstone using axisymmetric radial core floods and numerically modelling transport with various adsorption mechanisms.[56] They reported that only two-site or bilayer kinetic adsorption models could accurately describe the adsorption behaviour and could easily predict surfactant loss during EOR by surfactant flooding. The dynamic adsorption model can be best described by combining the time and space-dependent adsorption.[57,58] The aqueous surfactant transport is frequently written as an advection–dispersion–reaction equation (eqn (6)):[59]

$$\phi\frac{\partial C}{\partial t} + (1-\phi)\frac{\partial q}{\partial t} = D\frac{\partial^2 C}{\partial x^2} - v\frac{\partial C}{\partial x} \quad (6)$$

where ϕ is porosity, C is aqueous concentration, q is the adsorbed concentration, D is the dispersion coefficient, and v is pore velocity. The Langmuir isotherm was adopted as the equilibrium closure in the dynamic transport model due to its simplicity and common use in core-scale formulations. Dynamic adsorption is characterized by a linear driving-force kinetic model, wherein the adsorption rate is contingent upon the disparity between the instantaneous and equilibrium adsorbed quantities, with the equilibrium value ascertained from a Langmuir isotherm.[60,61]

2.10. Dynamic contact angle studies

The KRUSS DSA-25 model of a goniometer was used to measure the advancing contact angle by analyzing the droplet shape over time. The measurements were taken on 1 cm-thick pieces of sandstone and carbonate rock. These rock samples were oil-aged with crude oil at 85 °C. During contact angle measurement, a droplet of 100-ppm surfactant solution with around 20 μL was gently deposited on the rock surface, and the goniometer's high-resolution imaging system continuously recorded the droplet profile at 303 K.

3. Results and discussion

3.1. Static adsorption study

The adsorption characteristics of a series of nonionic, amine-based spacers, Gemini surfactants, were systematically evaluated on sandstone and carbonate rock samples. The adsorption behaviour of the synthesised Gemini surfactants over a prolonged time period has been observed; however, adsorption equilibrium was reached within 24 h, beyond which no further increase in adsorption occurred, as shown in Fig. S4 and S5. This study aimed to understand the influence of molecular structure, particularly the spacer length and number of amine groups, on surfactant adsorption behaviour in lithologies commonly encountered in enhanced oil recovery (EOR)

© 2026 The Author(s). Published by the Royal Society of Chemistry

Open Access Article. Published on 18 February 2026. Downloaded on 6/19/2026 8:10:42 PM.
This article is licensed under a Creative Commons Attribution-NonCommercial 3.0 Unported Licence.

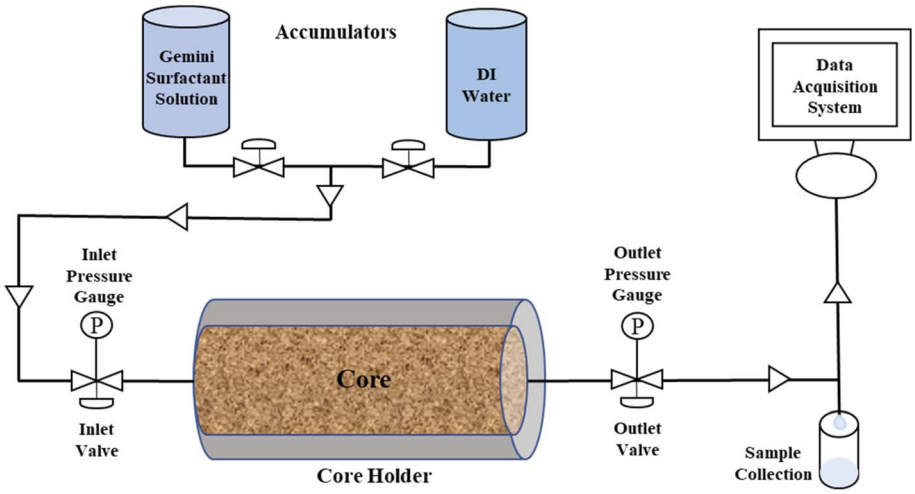

Fig. 3 Schematic of dynamic adsorption flooding system.

operations. The static adsorption experiments were conducted using finely ground rock powders, with prolonged equilibration to ensure equilibrium conditions and maximise surface accessibility. Therefore, the adsorption capacities obtained from this test provide equilibrium upper limits, whereas dynamic adsorption under flow conditions offers more reservoir-relevant retention behaviour.[59] The maxima were determined from the UV spectroscopy data for all the surfactants, as shown in Fig. 4.

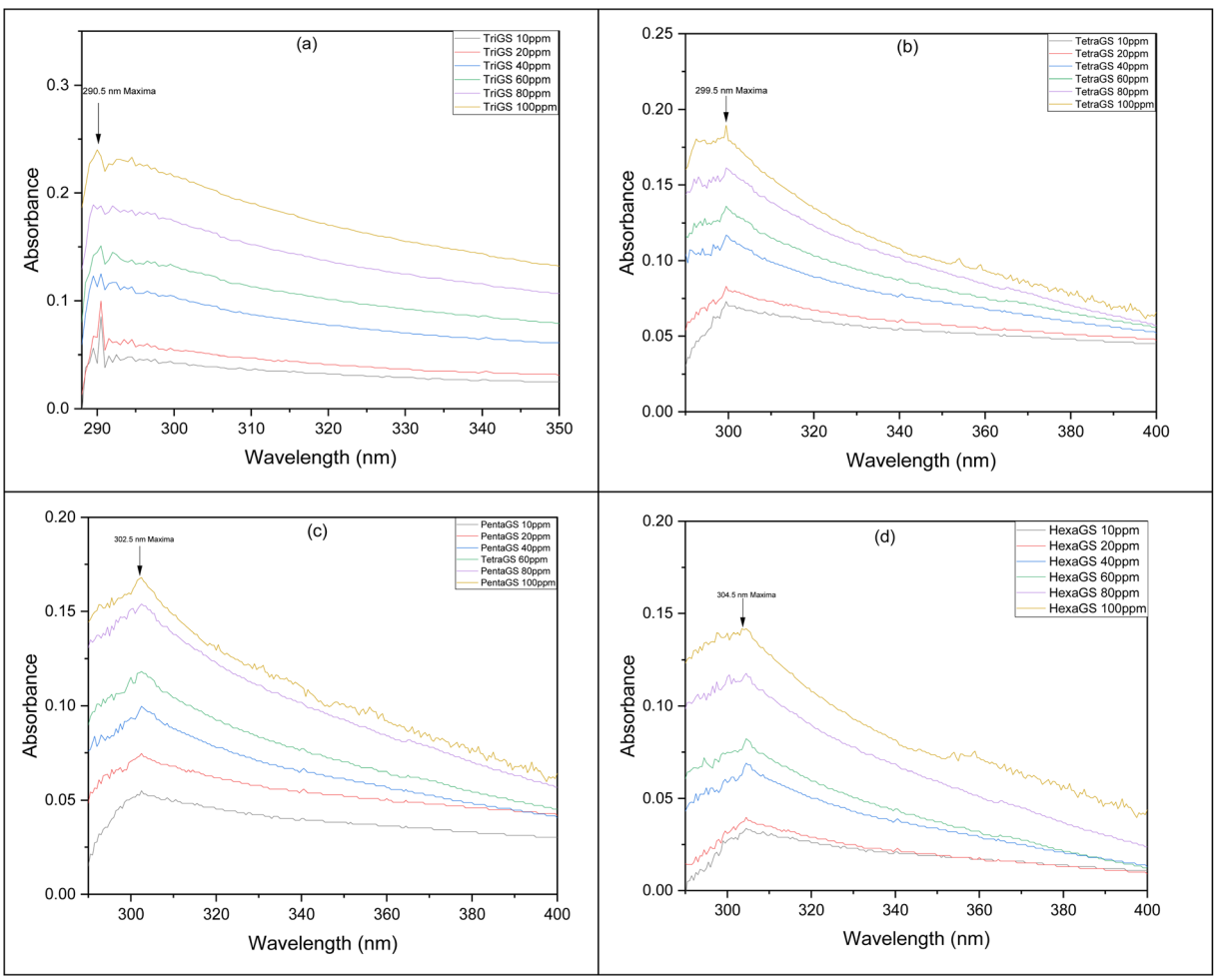

Fig. 4 Maxima determination of Gemini surfactants with the UV spectroscopy of different concentrations of surfactants (a) triamine GS, (b) tetramine GS, (c) pentamine GS, and (d) hexamine GS.

Open Access Article. Published on 18 February 2026. Downloaded on 6/19/2026 8:10:42 PM.
This article is licensed under a Creative Commons Attribution-NonCommercial 3.0 Unported Licence.

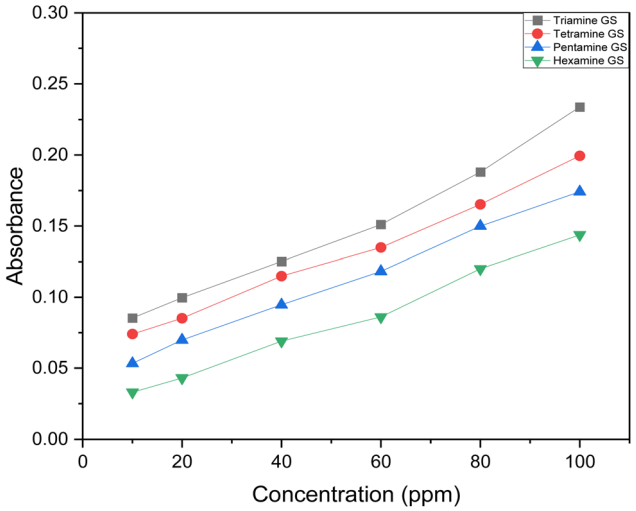

Fig. 5 Calibration curve of the initial absorbance value of Gemini surfactants at their respective maxima values.

A calibration curve for the synthesised Gemini surfactant was then plotted as shown in Fig. 5, to determine the adsorption of the Gemini surfactant.

After 24 hours of exposure, adsorption on sandstone ranged from 0.23 mg g^{-1} for Triamine GS to 0.072 mg g^{-1} for Hexamine GS, as shown in Fig. 6a. In carbonate rocks, adsorption was comparatively lower, with values ranging from 0.128 mg g^{-1} to 0.057 mg g^{-1}, as shown in Fig. 6b. These results highlight a clear trend, as the number of amine groups and the spacer length between them increased, the adsorption of the surfactants decreased.[50,62–64] This behaviour is attributed to the increased steric hindrance and enhanced hydrophilicity of surfactants with longer spacers and more terminal amine groups, which reduce their affinity for rock surfaces.[44,65,66] The nonionic nature of these surfactants further limits electrostatic interaction with the negatively charged mineral surfaces, particularly in carbonate formations that are typically less reactive than sandstone. The reduced adsorption of surfactants with longer spacer lengths, such as Hexamine GS, is especially favourable for EOR applications. Low adsorption minimizes surfactant retention within the reservoir, thus improving the chemical flooding efficiency and reducing overall operational costs. The molecular structure plays a crucial role in this context, longer carbon chains between the amine groups not only increase water solubility but also create a steric barrier that hinders close packing on rock surfaces.[11,41,42,67] Over a prolonged contact time of 15 days, all surfactants showed a negligible increase in adsorption. However, even at this stage, Hexamine GS consistently showed the least adsorption values on both rock samples. However, surfactants with extended spacer lengths and higher degrees of amine substitution, such as Hexamine GS, exhibit reduced adsorption tendencies, making them promising candidates for efficient and economical EOR formulations, especially in heterogeneous reservoirs.

The dependence of adsorption on spacer length can be described by changes in the molecular arrangement of Gemini surfactants at the rock oil interface. Surfactants with shorter spacers, such as Triamine and Tetramine GS, keep their two headgroups relatively close together, enabling stronger surface attachment and more efficient packing of available mineral adsorption sites. However, as the spacer length increases (Pentamine and Hexamine GS), the molecules become more flexible and sterically bulky. This leads to a larger hydrated interfacial structure, which hinders tight surface packing and reduces surfactant–surfactant association on the rock surface.[44,67] As a result, longer-spacer Gemini surfactants exhibit progressively lower adsorption, with Hexamine GS showing the lowest retention due to weaker interfacial packing and increased hydration.

3.2. Surface morphology analysis (FESEM)

Field Emission Scanning Electron Microscopy (FESEM) was employed to examine the surface morphology of sandstone and carbonate rock samples before and after treatment with the

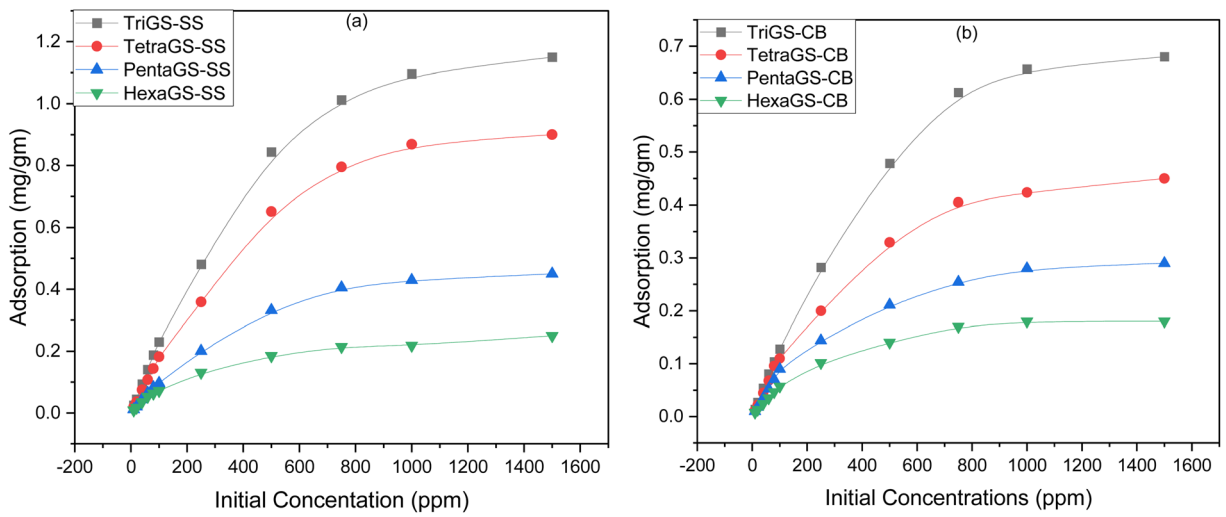

Fig. 6 Adsorption in mg per gm of Gemini surfactants onto (a) sandstone and (b) carbonate against the initial concentration.

© 2026 The Author(s). Published by the Royal Society of Chemistry

Open Access Article. Published on 18 February 2026. Downloaded on 6/19/2026 8:10:42 PM.
This article is licensed under a Creative Commons Attribution-NonCommercial 3.0 Unported Licence.

synthesized Hexamine Gemini surfactant (HexamineGS). The micrographs, captured at 250 00× magnification with a 200 nm scale bar, are presented in Fig. 7, enabling detailed observation of surface-level modifications resulting from surfactant adsorption.

The untreated sandstone sample (Fig. 7a) exhibits a highly irregular and rough surface composed of loosely packed, angular, and fragmented grains. The presence of sharp mineral edges and surface heterogeneity may influence surfactant–rock interactions. This morphology is typical of silicate-rich formations and indicates the sandstone's strong potential for surface interaction with amphiphilic molecules. Upon treatment with the Hexa GS surfactant, distinct surface modifications were observed in both rock types. The sandstone sample post-treatment (Fig. 7c) shows a noticeably smoother texture with partial masking of mineral grain boundaries and reduced sharpness. These changes were consistent with surface modification after surfactant treatment; however, FESEM contrast alone cannot unambiguously confirm an adsorbed molecular layer, since charging effects or residual deposition during drying may also contribute.

In contrast, the untreated carbonate surface (Fig. 7b) appears relatively smoother and more compact, with closely packed grains characteristic of calcite-dominated mineralogy. The uniform texture and reduced porosity imply fewer reactive sites and lower surface roughness, which may limit direct surfactant and rock interactions compared to sandstone.[68] The carbonate surface after surfactant treatment (Fig. 7d) exhibits less dramatic morphological alteration. A thin surface film and mild grain-boundary aggregation are visible, but the underlying mineral structure remains largely intact. This indicated comparatively less pronounced surface modification, potentially due to the smoother calcite-based matrix.[63,69]

Overall, FESEM analysis provided qualitative evidence of surface alteration consistent with adsorption trends, but was not interpreted as standalone proof of adsorption strength and was corroborated with UV-vis, EDX, and zeta potential measurements.

3.2.1. FESEM of sandstone. FESEM-EDX analysis of the sandstone sample, with and without treatment, has been performed to assess its semi-quantitative, surface-averaged elemental composition (Fig. S2 in the SI). The untreated sandstone primarily consisted of 46.1 wt% oxygen and 35.1 wt% silicon, reflecting its silicate-rich nature. The other components included 15.5 wt% carbon, with minor components including aluminium (3.9 wt%), iron (2.9 wt%), phosphorus (1.3 wt%), potassium (1.1 wt%), and other trace elements. Notably, nitrogen was absent in the untreated sample, confirming the absence of organic coatings or surfactant residues.

Following treatment with Hexamine GS, significant changes in surface chemistry were observed. An increased amount of carbon to 18.9 wt% with 3.1 wt% nitrogen was observed, suggesting adsorption of the organic surfactant layer. A marked increase in oxygen content to 50.2 wt% was also observed, likely due to oxygen-rich functional groups, such as the amide spacer group, present in the Gemini surfactant structure. In contrast, the concentrations of silicon, aluminium, and iron decreased to 25.6 wt%, 1.5 wt%, and 0.5 wt%, respectively, as shown in Table S2 in the SI. This decrease may reflect attenuation of the underlying mineral signal due to surface coverage or sample preparation effects. These elemental changes were considered only supportive evidence, since EDX provides semi-quantitative,

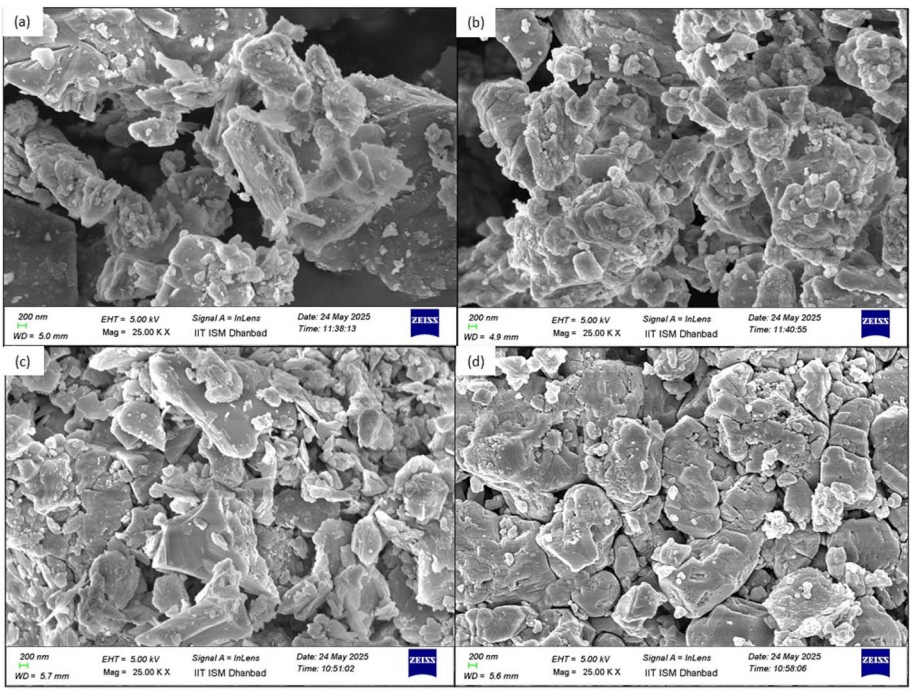

Fig. 7 FESEM images of (a) sandstone, (b) carbonate, (c) sandstone with hexa GS, and (d) carbonate with hexa GS, at 200 nm scale.

Open Access Article. Published on 18 February 2026. Downloaded on 6/19/2026 8:10:42 PM.
This article is licensed under a Creative Commons Attribution-NonCommercial 3.0 Unported Licence.

surface-averaged information and cannot distinguish between true adsorption and physically retained residues.[70,71]

3.2.2. FESEM of carbonate. FESEM-EDX analysis was also performed on carbonate rock samples to assess the changes in semi-quantitative, surface-averaged elemental composition before and after treatment with the Hexamine-based Gemini surfactant (Fig. S3, in the SI). The untreated carbonate primarily exhibited a high calcium content of 47.5 wt%, consistent with the calcite-rich composition typical of carbonate reservoirs. Oxygen was the next major component with 44.2 wt%, followed by 18.2 wt% carbon, and minor amounts of iron (1.8 wt%), copper (1.7 wt%), phosphorus (1.1 wt%), silicon (1.2 wt%), potassium (0.5 wt%), aluminium (0.7 wt%), and magnesium (0.2 wt%). As expected, nitrogen was absent in the untreated sample, confirming the absence of organic surfactant layers.

After surfactant treatment, noticeable changes were observed. A higher carbon content of 19.5 wt% with 2.7 wt% nitrogen was observed in sandstone samples, suggesting surface modification after the addition of the Hexamine Gemini surfactant to the carbonate surface. Oxygen content increased slightly to 46.4 wt%, which may be attributed to the oxygen-bearing functionalities within the surfactant structure, as shown in Table S3 in the SI. A decrease in calcium contribution to 32.5 wt% was observed, which may indicate signal attenuation due to surface-associated surfactant. Other elements, including silicon, phosphorus, potassium, aluminium, and copper, also showed decreased concentrations, further supporting the presence of an organic coating that altered the elemental visibility in EDX mapping.[71,72]

Both rock types exhibited elemental changes consistent with surfactant exposure; however, EDX results were interpreted as complementary support alongside UV-vis adsorption and electrokinetic measurements. However, the change in elemental concentration was more pronounced in sandstone, particularly concerning silicon, aluminium, and iron. This could be attributed to the higher surface reactivity and heterogeneous silicate composition of sandstone compared to the more homogeneous calcite-dominant carbonate matrix. These findings suggest stronger surfactant–rock interactions in sandstone, potentially enhancing its performance in wettability alteration and interfacial tension reduction for enhanced oil recovery (EOR) applications.

3.3. Surface charge measurements

Zeta potential measurements were carried out to gain qualitative insight into the electrokinetic behaviour of the Gemini surfactant systems in the presence of sandstone and carbonate rocks. It is important to note that zeta potential reflects the potential at the shear plane and is affected not only by changes in surface charge but also by solution properties such as ionic strength, dielectric constant, viscosity, and ion distribution. Therefore, the observed variations were interpreted as general indicators of interfacial modification rather than direct or quantitative evidence of adsorption or electrical double-layer compression.

Table 1 Zeta potential with and without addition of rock

Samples	GS solution	GS with sandstone	GS with carbonate
Zeta potential after 24 hours of mixing			
Tri GS	40.567	25.378	27.232
Tetra GS	45.991	26.897	29.679
Penta GS	50.9983	28.685	31.589
Hexa GS	52.7284	33.863	38.862
Zeta potential after 15 days of mixing			
Tri GS	40.567	23.437	25.957
Tetra GS	45.991	25.991	27.999
Penta GS	50.9983	27.489	29.044
Hexa GS	52.7284	31.232	37.650

After 24 h of mixing, a noticeable decrease in zeta potential was observed for all surfactant solutions upon contact with both rock types (Table 1). For instance, Triamine GS decreased from 40.567 mV in solution to 25.378 mV with sandstone and 27.232 mV with carbonate. Similarly, Hexamine GS, which showed the highest initial value (52.728 mV), decreased to 33.863 mV and 38.862 mV in the presence of sandstone and carbonate, respectively. These early-stage shifts were consistent with limited surfactant–mineral interactions, in agreement with the relatively low adsorption capacities measured over the same period.[62] With extended contact time up to 15 days, further reductions in zeta potential were observed across all surfactants, suggesting progressive changes in the interfacial environment over time.[73]

Moreover, the difference in zeta potential and adsorption between sandstone and carbonate systems may be influenced by differences in mineral surface charge characteristics and reactivity. The carbonate system showed comparatively higher zeta potential values than sandstone, attributed to differences in surface composition and ion release (*e.g.*, Ca^{2+} from calcite), which influence the interfacial structure and surfactant orientation. Additionally, increasing the spacer and hydrophobic chain length in the Gemini structure (from Triamine GS to Hexamine GS) resulted in higher initial zeta potential and lower adsorption rates at short contact times, consistent with steric hindrance and reduced accessibility.[74] However, over extended periods, these surfactants may have contributed to progressive interfacial modification, resulting in a significant reduction in zeta potential.

These electrokinetic results support the adsorption measurements, wettability alteration data, and dynamic core-flooding results. Overall, the observed trends underscore the coupled influence of surfactant structure, mineral type, and interaction duration on electrokinetic behaviour and adsorption dynamics, critical parameters in designing surfactant-based formulations for EOR and rock wettability alteration.

3.4. Static adsorption isotherm modelling

The adsorption behaviour profiles of mustard oil-derived Gemini surfactants on sandstone and carbonate were quantitatively analyzed and modelled using multiple equilibrium isotherm models, specifically Linear, Langmuir, Freundlich,

© 2026 The Author(s). Published by the Royal Society of Chemistry

Open Access Article. Published on 18 February 2026. Downloaded on 6/19/2026 8:10:42 PM.
This article is licensed under a Creative Commons Attribution-NonCommercial 3.0 Unported Licence.

Table 2 Adsorption isotherm parameter of surfactant on both rock surfaces

Adsorbent			Sandstone				Carbonate			
Surfactant			Tri	Tetra	Penta	Hexa	Tri	Tetra	Penta	Hexa
Models	Linear isotherm	K_H	1.3×10^{-3}	1.0×10^{-3}	0.5×10^{-3}	0.2×10^{-3}	0.7×10^{-3}	0.5×10^{-3}	0.3×10^{-3}	0.2×10^{-3}
		C	1.2×10^{-3}	1.7×10^{-3}	3.1×10^{-3}	4.9×10^{-3}	2.5×10^{-3}	0.5×10^{-3}	0.2×10^{-3}	2.3×10^{-3}
		R^2	0.9998	0.9993	0.9922	0.9781	0.9986	0.9934	0.9989	0.9999
	Langmuir isotherm	K_L	2.15×10^{-3}	2.21×10^{-3}	2.35×10^{-3}	3.62×10^{-3}	2.04×10^{-3}	2.57×10^{-3}	3.15×10^{-3}	3.52×10^{-3}
		q_0	1.57	1.258	0.610	0.291	0.972	0.592	0.360	0.225
		R^2	0.9908	0.9964	0.9991	0.9999	0.9974	0.9992	0.9997	0.9998
	Freundlich isotherm	K_F	2.75×10^{-2}	1.93×10^{-2}	1.06×10^{-2}	0.91×10^{-2}	1.33×10^{-2}	1.17×10^{-2}	0.94×10^{-2}	0.69×10^{-2}
		n_F	1.87	1.82	1.87	2.15	1.78	1.93	2.06	2.15
		R^2	0.9641	0.9773	0.9921	0.9978	0.9845	0.9931	0.9969	0.9973
	Redlich–Peterson isotherm	K_R	3.07×10^{-3}	2.06×10^{-3}	1.12×10^{-3}	1.13×10^{-3}	1.44×10^{-3}	1.34×10^{-3}	1.06×10^{-3}	0.598×10^{-3}
		α_r	0.192×10^{-3}	0.0501×10^{-3}	0.146×10^{-3}	5.65×10^{-3}	0.0246×10^{-3}	0.874×10^{-3}	1.79×10^{-3}	0.344×10^{-3}
		β_r	1.32	1.48	1.34	0.95	1.56	1.13	1.07	1.28
		R^2	0.9994	0.9994	0.9998	0.9998	0.9998	0.9995	0.9996	0.9997
	Hill isotherm	K_H	1042.5	1184.21	914.84	236.78	1584.32	613.57	680.00	650.00
		n_H	1.228	1.226	1.183	0.951	1.271	1.103	1.229	1.115
		q_{SH}	1.348	1.082	0.539	0.30	0.812	0.56	0.30	0.24
		R^2	0.9981	0.9979	0.9994	0.9999	0.9988	0.9993	0.9996	0.9987

Redlich–Peterson, and Hill isotherm models. The experimental data were fitted to these models, and the corresponding parameters are summarized in Table 2.

3.4.1. Linear adsorption isotherm. The Linear isotherm provided an excellent fit for all surfactants with very high correlation coefficients, but only for low concentrations of 100 ppm, after that, the R^2 ranged from 0.8447 to 0.8461. The low Henry's constants (K_H) obtained for Hexamine GS of 0.2×10^{-3} L mg^{-1} for both sandstone and carbonate confirm the minimal adsorption tendency of Hexamine GS relative to shorter spacer length surfactants of Triamine, Tetramine and Pentamine GS. This linear behaviour suggests that the weak affinity of longer spacer length Gemini surfactants towards mineral surfaces occurs in regions where adsorption sites remain largely unsaturated with dilute systems of GS.[75–77] The adsorption behaviour of the Gemini surfactants, evaluated with different spacer lengths and concentrations on both sandstone and carbonate rock samples, was modelled using the Linear isotherm, as shown in Fig. 8.

3.4.2. Langmuir isotherm. The Langmuir model, which assumes monolayer adsorption onto homogeneous surfaces, also described the data well with R^2 values in the range of 0.990–0.9999. The maximum adsorption capacities (q_0) decreased systematically with increasing spacer length, from 1.57 mg g^{-1} for Triamine GS to 0.291 mg g^{-1} for Hexamine GS on sandstone, and from 0.972 mg g^{-1} to 0.225 mg g^{-1} on carbonate. This trend of maximum adsorption capacities (q_0) demonstrates that steric hindrance and enhanced hydrophilicity associated with longer polyamine spacers reduce molecular packing density at the rock–fluid interface. However, Hexamine GS consistently exhibited the lowest monolayer capacity, which is highly favourable for EOR since lower adsorption minimizes surfactant loss during chemical flooding.[44,77] The experimental data for adsorption at varying spacer lengths and concentrations on both rock samples for Gemini surfactants were plotted and fitted to the Langmuir isotherm model, as shown in Fig. 9.

3.4.3. Freundlich isotherm. The Freundlich model, which describes multilayer adsorption on heterogeneous surfaces, also fits strongly with R^2 ranging from 0.9641 to 0.9978 on sandstone and 0.9845 to 0.9973 on carbonate with increasing spacer length. The Freundlich surface heterogeneity factor (n_F) was >1 in all cases, indicating favourable adsorption. However, higher values of n_F 2.15 for Hexamine GS than other shorter spacer length GS suggests weaker surface-specific binding and shows a tendency of reversible adsorption toward longer-spacer surfactants. This fitting again confirms that molecular architecture strongly modulates adsorption affinity.[65,67] Fig. 10 shows the adsorption behaviour of the synthesized Gemini surfactants at varying spacer lengths and concentrations on both rock samples, fitted to the Freundlich isotherm model.

3.4.4. Redlich–Peterson isotherm. The Redlich–Peterson model, a hybrid of both Langmuir and Freundlich characteristics, although Langmuir and Freundlich models were commonly used, adsorption on actual reservoir rocks did not occur on perfectly homogeneous surfaces. Both sandstone and carbonate substrates exhibited mineralogical heterogeneity, surface irregularities, and non-uniform adsorption energies.

© 2026 The Author(s). Published by the Royal Society of Chemistry

Open Access Article. Published on 18 February 2026. Downloaded on 6/19/2026 8:10:42 PM.
This article is licensed under a Creative Commons Attribution-NonCommercial 3.0 Unported Licence.

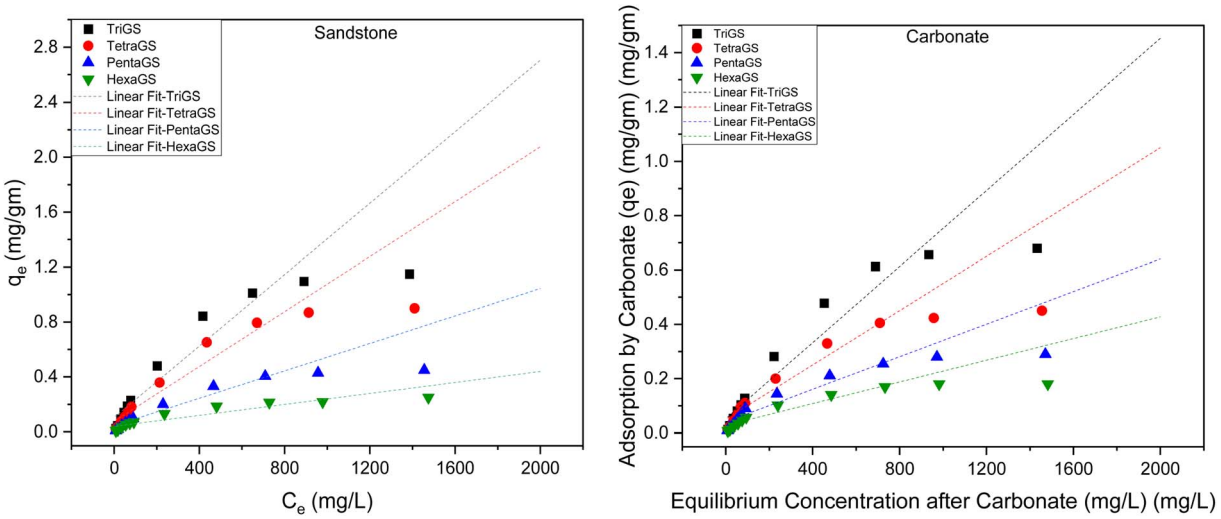

Fig. 8 An extended curve for the linear isotherm of both rock samples.

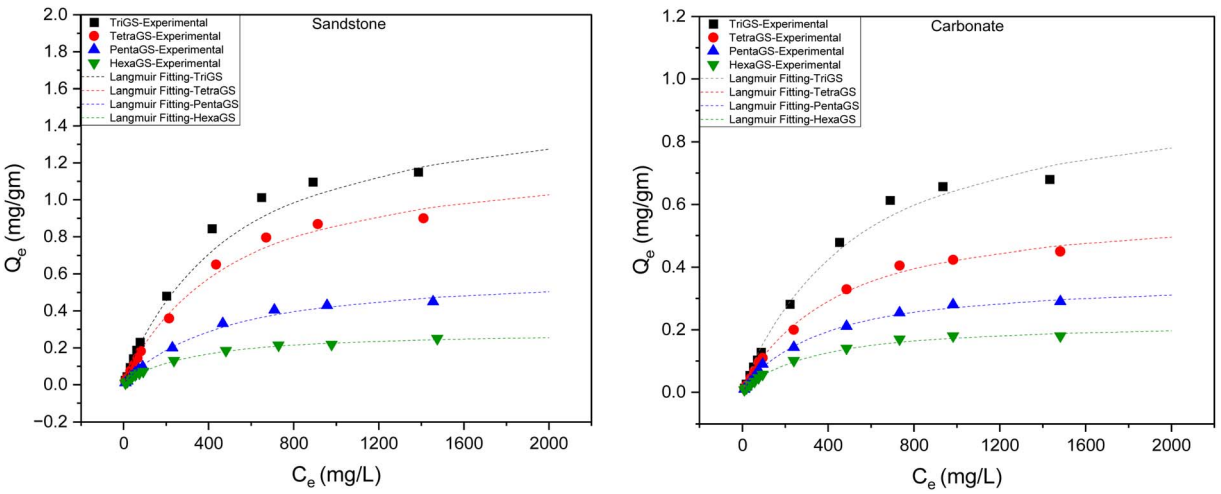

Fig. 9 Langmuir adsorption isotherm fitting curves of both rock samples.

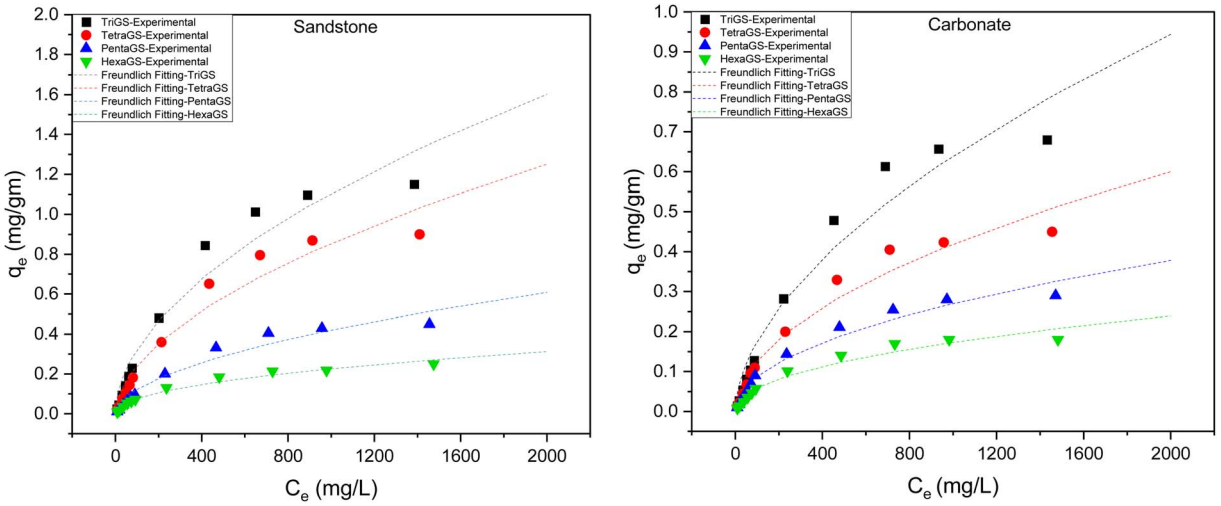

Fig. 10 Freundlich adsorption isotherm fitting curves of both rock samples.

© 2026 The Author(s). Published by the Royal Society of Chemistry

Open Access Article. Published on 18 February 2026. Downloaded on 6/19/2026 8:10:42 PM.
This article is licensed under a Creative Commons Attribution-NonCommercial 3.0 Unported Licence.

Therefore, the Redlich–Peterson model was considered more physically appropriate in this study because it combined Langmuir-type site saturation with Freundlich-type heterogeneity. This allowed it to describe adsorption behaviour that shifted from near-monolayer coverage at lower concentrations to more heterogeneous surface interactions at higher concentrations. Such hybrid behaviour was particularly relevant for Gemini surfactants adsorbing onto complex porous mineral surfaces.[37,78] This model provided the best overall fit to the adsorption data, with $R^2 > 0.999$ across all GS. The $\beta_r$values ranging from 0.95 to 1.56 confirm that adsorption was intermediate between ideal monolayer and heterogeneous multilayer processes. Alongside, the low K_R values obtained of 1.13×10^{-3} L mg^{-1} for sandstone and 0.598×10^{-3} L mg^{-1} for carbonate for Hexamine GS reflect reduced interaction strength with mineral surfaces. This hybrid model outcome suggests that while initial adsorption may follow monolayer coverage, additional multilayer formation can be possible, particularly for shorter-spacer molecules.[79,80] The adsorption behaviour of Gemini surfactants, assessed at varying spacer lengths and concentrations on both rock samples, was modelled using the Redlich–Peterson isotherm, as seen in Fig. 11.

3.4.5. Hill isotherm. The Hill isotherm model, which describes cooperative adsorption effects, was also considered in this study because Gemini surfactants contain two headgroups linked by a spacer, which could promote intermolecular association and surface clustering during adsorption. Such molecular architectures could lead to cooperative or competitive binding behaviour, in which the adsorption of one molecule influences the affinity of subsequent adsorption events. In the present work, Hill coefficient values close to unity suggested that adsorption was largely non-cooperative, whereas slight deviations observed for longer spacer surfactants indicated reduced packing efficiency and weak negative cooperativity. Therefore, the Hill model provided additional mechanistic insight into the influence of Gemini surfactant structure beyond simple equilibrium fitting.[81,82] Although this model also provided excellent fits to the experimental data, with R^2 values up to 0.9999 for Hexamine GS. The Hill coefficients (n_H) were close to unity for all systems, indicating predominantly non-cooperative binding. However, a slight deviation of n_H, of 0.951 from unity for sandstone for Hexamine GS, implies weak negative cooperativity, where adsorption of one molecule slightly reduces the prospect of following adsorption. This behaviour further supports the reduced packing efficiency of longer-spacer Gemini surfactants.[4,82] Fig. 12 illustrates the Hill isotherm fitting of adsorption data for Gemini surfactants with different spacer lengths and concentrations on both rock samples.

The static isotherm modelling analysis demonstrates that adsorption of Gemini surfactants onto both sandstone and carbonate was strongly dependent on spacer length, with adsorption decreasing systematically from Triamine to Hexamine GS as the spacer length increases. The excellent fits across different models suggest a mixed adsorption mechanism involving both monolayer and heterogeneous multilayer processes.[83] The consistently low adsorption parameters for Hexamine GS highlight its potential for chemical EOR, as reduced retention leads to improved surfactant utilization, cost-effectiveness, and less harm to the environment.

The fitted parameters in Table 2 provide mechanistic insight into the adsorption process. The decrease in Langmuir monolayer capacity (q_0) from Triamine to Hexamine GS confirmed reduced surface packing with increasing spacer length. Freundlich constants further suggested that adsorption remained partially reversible on heterogeneous mineral sites. The strong Redlich–Peterson fit indicated mixed-mode adsorption on real reservoir surfaces, while Hill coefficients close to unity supported largely non-cooperative binding. Together, these results demonstrated that spacer length governed adsorption through steric and hydration-controlled packing effects rather than strong chemisorption.[37,44,67]

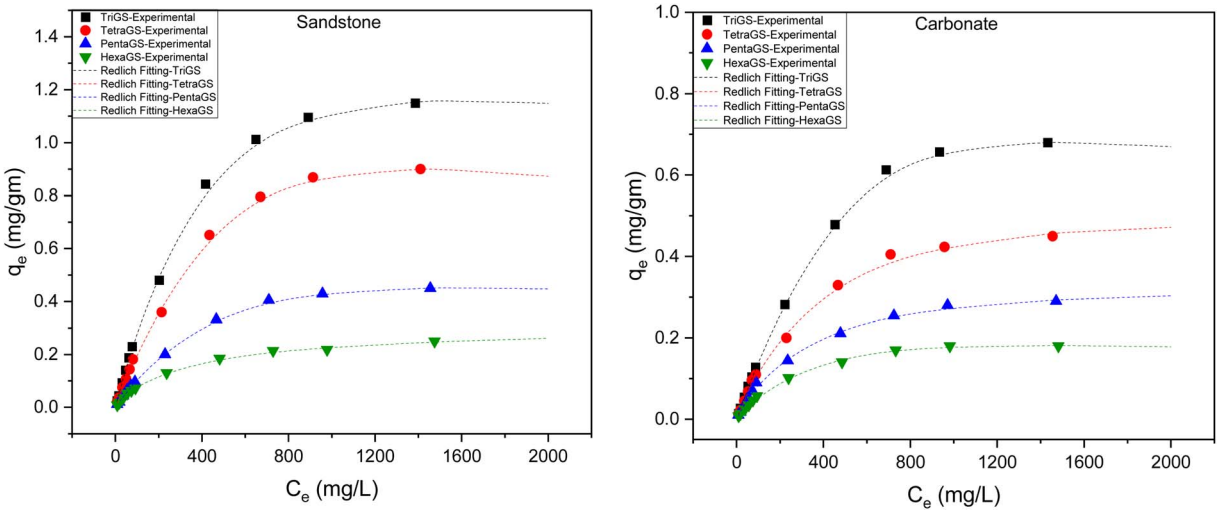

Fig. 11 Redlich–Peterson isotherm fitting curves of both rock samples.

Open Access Article. Published on 18 February 2026. Downloaded on 6/19/2026 8:10:42 PM.
This article is licensed under a Creative Commons Attribution-NonCommercial 3.0 Unported Licence.

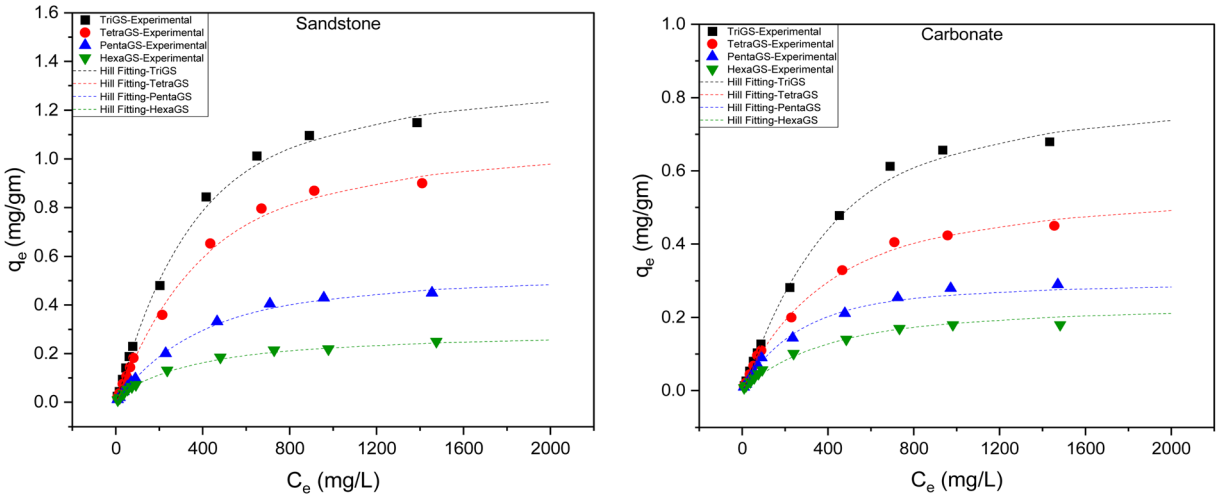

Fig. 12 Hill isotherm fitting curves of both rock samples.

3.5. Kinetic adsorption modelling

The experimental kinetic data were analyzed using pseudo-first-order, pseudo-second-order, and intra-particle diffusion models were applied to understand the adsorption mechanisms with the adsorption rate of Gemini surfactants derived from mustard oil. The parameters that control the adsorption rate are indicated by the calculated rate constants, equilibrium adsorption capacities, and the R^2 fit values, as shown in Table 3.

3.5.1. Pseudo first order. The pseudo-first-order model showed excellent fitting with the experimental data, with R^2 values ranging from 0.9937 to 0.9987 across all GS. The computed equilibrium adsorption capabilities (q_e) closely aligned with the experimental findings, as for sandstone, where Triamine GS demonstrated q_e of 0.286 mg g^{-1}, in contrast to 0.088 mg g^{-1} for Hexamine GS. The results showed the same trends as in static models in carbonate, with q_e declining systematically from 0.171 mg g^{-1} for Triamine GS to 0.070 mg g^{-1} for Hexamine GS (Fig. 13). The diminishing q_e values with extended spacer length further emphasize the reduced adsorption affinity of Gemini surfactants with longer spacers. The correlation coefficients indicate that the adsorption kinetics are primarily governed by diffusion-controlled physical adsorption, for Gemini surfactants on mineral surfaces.[66,77,84]

Although the pseudo-first-order kinetic model suggested that diffusion-controlled physisorption was the dominant adsorption pathway, this behaviour did not exclude the presence of weak specific interactions. In particular, the amide and polyamine functionalities present in the synthesized Gemini surfactants could have contributed through hydrogen bonding, dipole–dipole interactions, or mild surface complexation with surface hydroxyl groups in sandstone and carbonate functional sites. Therefore, the adsorption process was best described as predominantly physical in nature, supplemented by weak chemisorptive contributions rather than irreversible chemical binding[85,86]

3.5.2. Pseudo second order. The pseudo-second-order model also yielded a good fit, although the R^2 values ranged from 0.9903 to 0.9969, which were marginally inferior to those of the pseudo-first-order model (Fig. 14). This indicates that although chemisorption activities by electron exchange between surfactant head groups and active mineral surfaces may occur to a certain degree, but they were not the predominant mechanism in our GS system. The rate constants (K_2) exhibited a considerable increase with spacer length, with values of 19.30 $\times$ 10^{-1} g mg^{-1} h^{-1} for Hexamine GS on sandstone and 19.37 $\times$ 10^{-1} g mg^{-1} h^{-1} on carbonate, which signifies a more rapid equilibrium achievement for molecules

Table 3 Kinetics adsorption parameter of surfactant on both rock surfaces

Adsorbent			Sandstone				Carbonate			
Surfactant			Tri	Tetra	Penta	Hexa	Tri	Tetra	Penta	Hexa
Models	Pseudo first order	K_1	9.5×10^{-2}	9.1×10^{-2}	8.79×10^{-2}	8.3×10^{-2}	7.0×10^{-2}	7.02×10^{-2}	8.38×10^{-2}	9.3×10^{-2}
		q_e	0.286	0.221	0.121	0.088	0.171	0.146	0.115	0.070
		R^2	0.9965	0.9981	0.9982	0.9937	0.9981	0.9954	0.9987	0.9984
	Pseudo-second order	K_2	4.61×10^{-1}	6.53×10^{-1}	13.3×10^{-1}	19.30×10^{-1}	8.35×10^{-1}	9.32×10^{-1}	11.69×10^{-1}	19.37×10^{-1}
		q_e	0.246	0.192	0.102	0.076	0.135	0.119	0.097	0.062
		R^2	0.9903	0.9916	0.9950	0.9969	0.9939	0.9933	0.9929	0.9923
	Intra-particle diffusion model	K_{id}	5.97×10^{-2}	4.64×10^{-2}	2.55×10^{-2}	1.76×10^{-2}	3.32×10^{-2}	2.91×10^{-2}	2.34×10^{-2}	1.46×10^{-2}
		R^2	0.9905	0.9929	0.9867	0.9974	0.9904	0.9905	0.9921	0.9943

© 2026 The Author(s). Published by the Royal Society of Chemistry

Open Access Article. Published on 18 February 2026. Downloaded on 6/19/2026 8:10:42 PM.
This article is licensed under a Creative Commons Attribution-NonCommercial 3.0 Unported Licence.

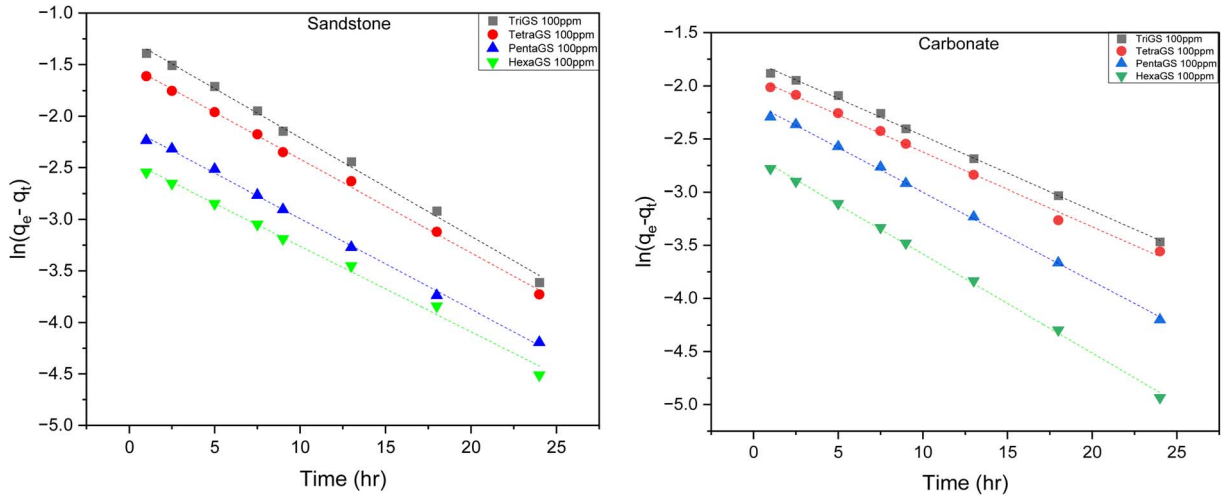

Fig. 13 The adsorption study of HexaGS surfactant by pseudo-first order kinetics of both rock samples.

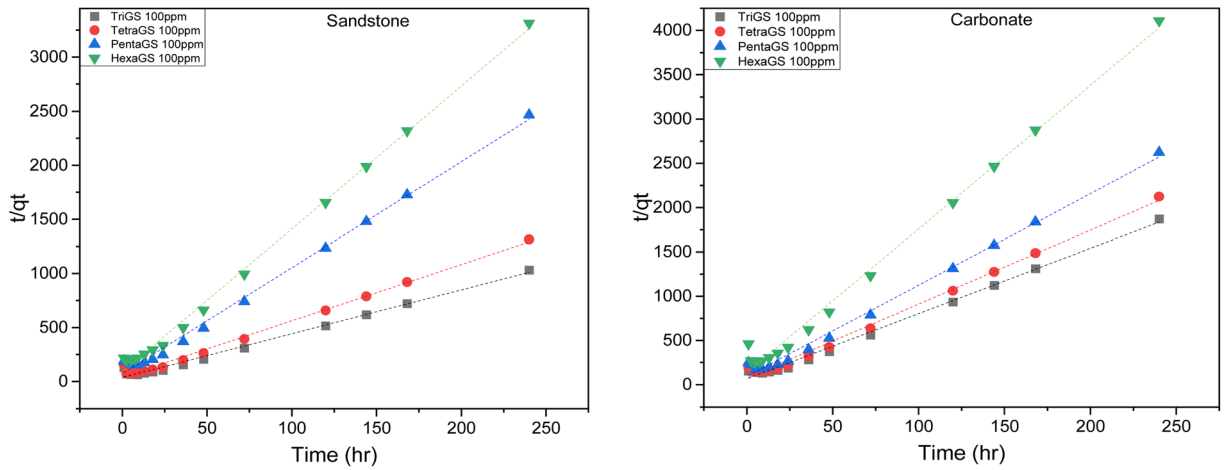

Fig. 14 The adsorption study of HexaGS surfactant by pseudo-second order kinetics of both rock samples.

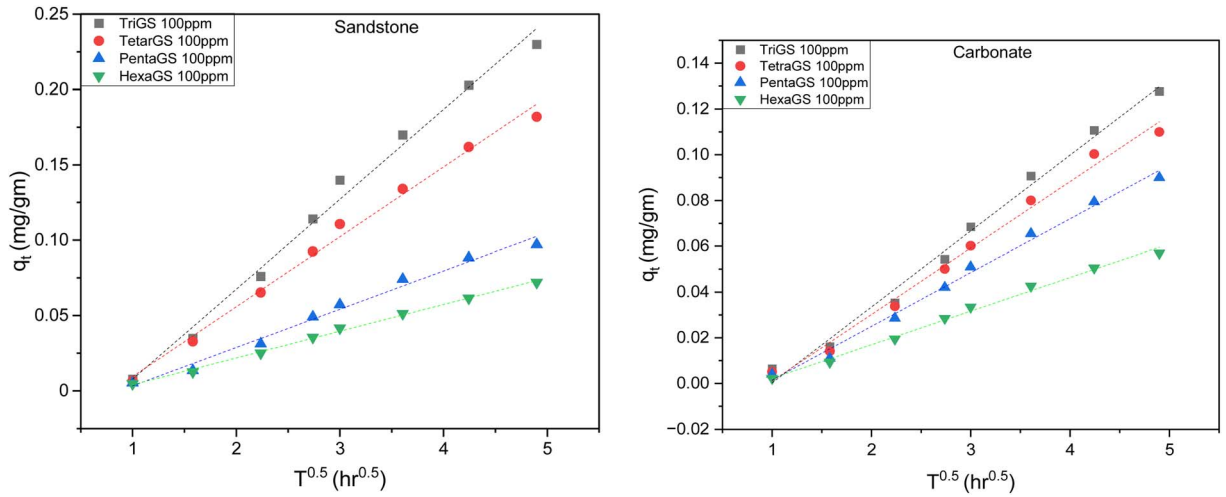

Fig. 15 The adsorption study of HexaGS surfactant by intra-particle diffusion kinetics of both rock samples.

Open Access Article. Published on 18 February 2026. Downloaded on 6/19/2026 8:10:42 PM. This article is licensed under a Creative Commons Attribution-NonCommercial 3.0 Unported Licence.

with longer spacers.[84] This trend indicates the diminished adsorption ability of longer-spacer surfactants, facilitating a more rapid attainment of equilibrium due to a reduced number of possible binding contacts.[87]

3.5.3. Intra-particle diffusion model. The intra-particle diffusion model was additionally employed to assess the role of pore diffusion in the adsorption process (Fig. 15). The intra-particle diffusion constants (K_{id}) exhibited a consistent decline with the elongation of the spacer length, decreasing from 5.97 $\times 10^{-2}$ mg g^{-1} h$^{-1/2}$ for Triamine GS to 1.76 $\times 10^{-2}$ mg g^{-1} h$^{-1/2}$ for Hexamine GS, in sandstone, and from 3.32 $\times 10^{-2}$ mg g^{-1} h$^{-1/2}$ to 1.46 $\times 10^{-2}$ mg g^{-1} h$^{-1/2}$ on carbonate. The R^2 values ranging from 0.9867 to 0.9974 suggest that intra-particle diffusion influences the overall kinetics, and the non-zero intercepts affirm that film diffusion and surface adsorption were also significant factors.[84] The adsorption of Gemini surfactants onto sandstone and carbonate occurs *via* a multi-step kinetic process, initially governed by boundary-layer diffusion and surface contacts, subsequently transitioning to slow intra-particle diffusion into the pore structure.[67,79]

3.6. Thermodynamic analysis

The Gibbs free energy change of adsorption was determined for the adsorption of mustard oil-derived Gemini surfactants onto sandstone and carbonate at a concentration of 100 ppm. All ΔG values were negative, varying from −18.038 to −19.859 kJ mol^{-1}, indicating that the adsorption of Gemini surfactants onto both rock types was spontaneous at 303 K at a specific concentration of 100 ppm, as shown in Table 4. The magnitude of ΔG offers critical insight into the adsorption mechanism, where the values between −20 and 0 kJ mol^{-1} are indicative of physisorption, characterized by electrostatic interactions, hydrogen bonding, or van der Waals forces, while values more negative than −40 kJ mol^{-1} generally signify chemisorption, characterized by robust covalent bonding or ion exchange.[53,75] The measured ΔG values ranged from −18.038 to −19.859 kJ mol^{-1} in this study, which can be associated with the physisorption, characterized by physical interactions between the surfactant head groups and the functional groups of the mineral surface. This insight validates the kinetic study, wherein pseudo-first-order models exhibited superior fitting relative to pseudo-second-order, hence reinforcing the pre-eminence of physisorption.[44,87]

The magnitude of ΔG became increasingly negative with longer spacer lengths, decreasing from −18.17 kJ mol^{-1} for Triamine GS to −19.86 kJ mol^{-1} for Hexamine GS in the sandstone sample, and from −18.038 to −19.788 kJ mol^{-1} in the carbonate sample. This tendency suggests that longer-spacer Gemini surfactants exhibit more favourable interactions with rock surfaces, although through mild physical pressures.[88] The increase of spontaneity with spacer length may be ascribed to tailored molecular flexibility and superior conformational adaptation of Hexamine GS at the rock and liquid interface, promoting stronger hydrophobic interactions and greater alignment of head groups with mineral surface sites. In the comparison of rock types, adsorption on carbonate surfaces consistently shows larger negative ΔG values than sandstone for Tetramine GS and Pentamine GS. This indicates the enhanced electrostatic interaction between the Gemini head groups and the charged carbonate sites for these specific surfactants.[67,79]

3.7. Dynamic adsorption and desorption study

Dynamic adsorption experiments were performed on sandstone and carbonate core samples to evaluate the retention and displacement efficiency of Hexamine GS. Fig. 16 and 17 illustrate the adsorption–desorption concentration profiles, which show the effluent concentration *versus* injected pore volumes profile and the associated adsorption capacity curves, respectively. These curves illustrate the association between adsorption in mg g^{-1} per rock and pore volumes.

During the initial injection phase from 0 to 2.5 PV, the effluent surfactant concentration was minimal for both sandstone and carbonate samples, indicating a strong initial absorption of Hexamine GS on both rock surfaces. As the injection continued, the effluent concentration progressively increased, indicating the eventual saturation of the adsorption sites in rock samples. A breakthrough occurred at approximately 6 to 8 pore volumes for sandstone and 5 to 7 pore volumes for carbonate, after which effluent concentrations increased significantly towards the injected concentration of 100 ppm. A steady-state plateau of approx. 100 ppm concentration was attained after approximately 10 to 13 PVs in both systems, indicating that adsorption equilibrium was established during this interval.[44,77]

The dynamic adsorption capacity curves exhibited a rapid rise during the initial process volumes, aligning with the occupation of rock surface sites, followed by a progressive plateau as the system neared equilibrium. The maximum dynamic adsorption for sandstone was approximately 0.013 mg g^{-1}, and for carbonate, it was approximately 0.0087 mg g^{-1}, prior to the desorption procedure, which involved flooding with distilled water.

The much lower adsorption observed in the dynamic core-flooding experiments compared with the static adsorption tests was mainly attributed to flow-related transport effects and limited contact time. In the static adsorption studies, surfactant

Table 4 The Gibbs free energy (ΔG) of the adsorption of the synthesized Gemini surfactant

Rock samples	Sandstone				Carbonate			
Surfactants	Triamine GS	Tetramine GS	Pentamine GS	Hexamine GS	Triamine GS	Tetramine GS	Pentamine GS	Hexamine GS
ΔG (kJ mol^{-1})	−18.170	−18.406	−18.668	−19.859	−18.038	−18.787	−19.406	−19.788

© 2026 The Author(s). Published by the Royal Society of Chemistry

Open Access Article. Published on 18 February 2026. Downloaded on 6/19/2026 8:10:42 PM.
This article is licensed under a Creative Commons Attribution-NonCommercial 3.0 Unported Licence.

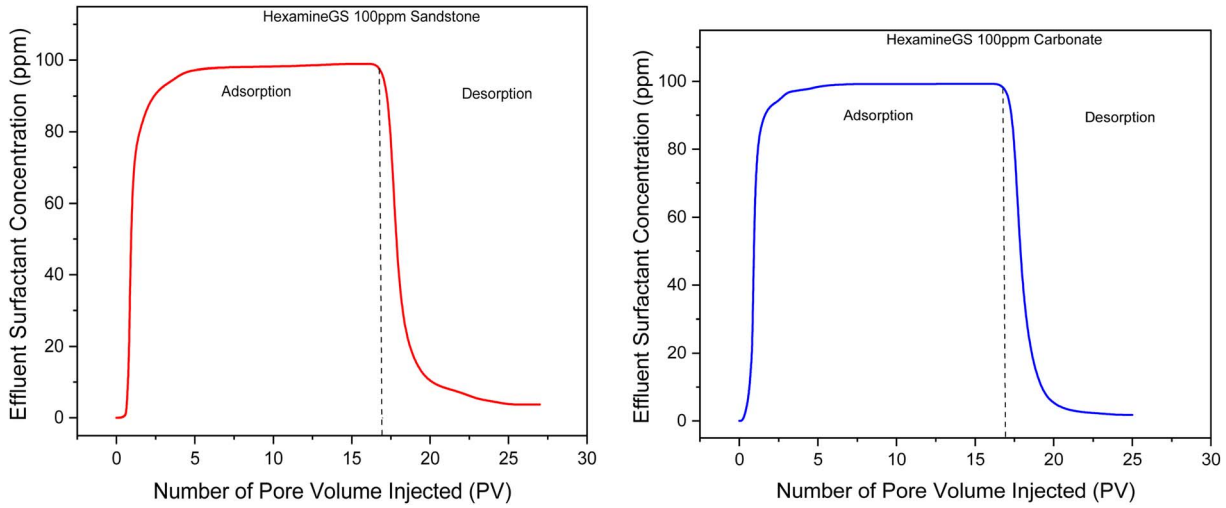

Fig. 16 Adsorption–desorption concentration profile of Hexamine GS of sandstone and carbonate rock samples.

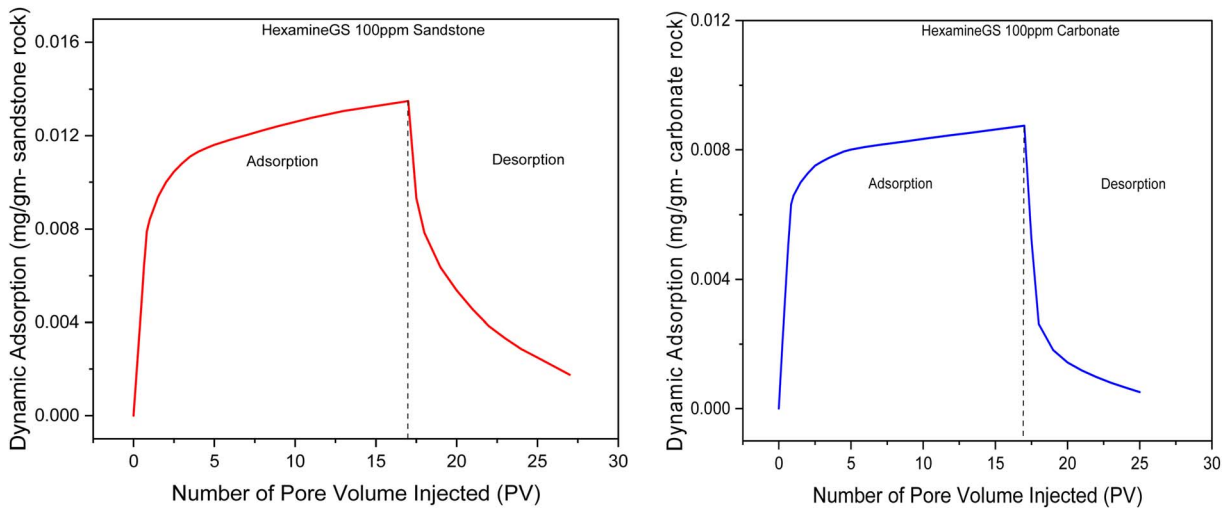

Fig. 17 Dynamic adsorption profile of Hexamine GS of sandstone and carbonate rock samples.

molecules remained in prolonged contact with finely crushed rock surfaces, allowing the system to approach equilibrium conditions and enabling multilayer adsorption to develop over 24 hours. Under dynamic flooding, however, surfactant transport occurred through intact porous media, where the residence time inside the core was relatively short, and adsorption became strongly influenced by mass-transfer limitations. In addition, not all mineral surface sites were equally accessible under flow because pore-throat restrictions limited surfactant diffusion into smaller pore regions. Continuous hydrodynamic dispersion during injection also promoted partial desorption and redistribution of weakly bound molecules.[87] Consequently, dynamic adsorption more realistically represented reservoir-scale retention under flowing conditions, yielding adsorption values that were typically much lower than those obtained under static equilibrium conditions.[59]

Despite the fact that carbonate rocks typically exhibit enhanced electrostatic interactions with surfactants, the diminished adsorption observed in carbonate cores relative to sandstone suggests a reduced retention of Hexamine GS in carbonate lithologies. The diminished retention may be attributed to the elongated hexamine spacer in the Gemini surfactant, which enhances molecular flexibility and steric hindrance, thereby decreasing effective packing density on the mineral surface.[80,89,90]

The desorption phase further emphasized the reversibility of the adsorption. Upon transitioning to surfactant-free slug at approximately 16 PV, the effluent concentration decreased rapidly, alongside a gradual reduction in predicted dynamic adsorption. Desorption was far more evident in carbonate samples, where the adsorbed surfactant diminished nearly entirely within approximately 10 pore volumes after distilled water injection, whereas sandstone retained a minor residual component. This suggests that the adsorption of Hexamine GS is predominantly reversible and governed by physical interactions rather than irreversible chemisorption, in accordance

Open Access Article. Published on 18 February 2026. Downloaded on 6/19/2026 8:10:42 PM.
This article is licensed under a Creative Commons Attribution-NonCommercial 3.0 Unported Licence.

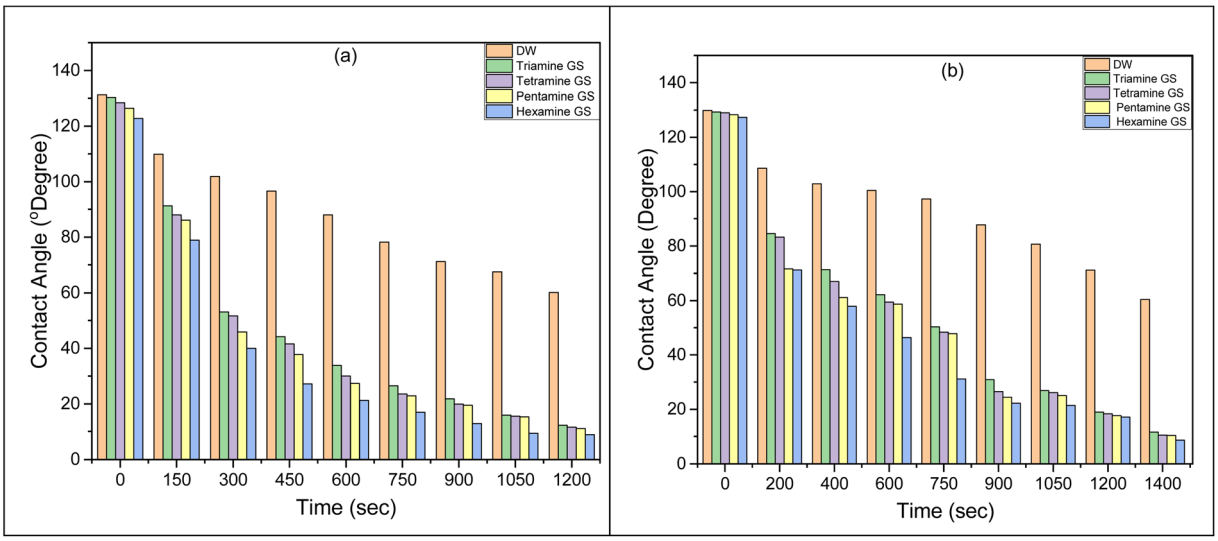

Fig. 18 The contact angle measurements with time for (a) sandstone and (b) carbonate rock samples.

with the thermodynamic analysis, where ΔG was approximately -19.859 kJ mol^{-1} in sandstone and -19.788 kJ mol^{-1} in carbonate.[30,91]

The dynamic adsorption–desorption behaviour demonstrates that Hexamine GS has minimal retention, quick breakthrough, and high desorption efficiency in both cores. These attributes are beneficial for EOR operations because they reduce surfactant depletion during flooding. The findings further substantiate the conclusions derived from static adsorption, adsorption kinetics, and thermodynamic evaluations, indicating that longer-spacer Gemini surfactants are more effective choices for chemical flooding in both reservoirs.

3.8. Dynamic contact angle studies

The capacity of all four synthesized Gemini surfactants to alter wettability was assessed for both sandstone and carbonate reservoir rocks at their critical micelle concentration, as illustrated in Fig. 18a and b, respectively. The incorporation of Tri, Tetra, Penta, and Hexamine GS at 100 ppm leads to a decrease in the dynamic contact angle of approximately 79%, 81%, 82%, and 85%, within 12 minutes in sandstone and 78%, 80%, 81%, and 83% within 15 minutes in carbonate, while comparing with distilled water. Because silicate minerals (SiO_2) have negatively charged properties, the surface properties of sandstone have an impact on the wettability modification of sandstone reservoirs. Van der Waals forces and hydrogen bonds are the primary mechanisms by which sandstone rocks interact with nonionic GS.[92] Nonionic Gemini surfactants adsorb efficiently onto mineral surfaces through their paired head groups and hydrophobic chains, reducing the surface affinity for crude oil. This adsorption lowers surface energy, promotes rock hydrophilicity, and supports the formation of a stable water layer that prevents oil from reattaching.[65] In carbonate formations, nonionic Gemini surfactants modify wettability by adsorbing onto mineral surfaces through hydrogen bonding and van der Waals interactions. This weakens the attachment of crude oil, lowers surface energy, and promotes a transition from oil-wet to water-wet conditions.[93] The reduced surface energy and the formation of a water-compatible layer further support the alteration of wettability. By binding water molecules, the surfactant head groups create a stable film that inhibits the return of oil to the rock surface.[4,45] In both rock types, reducing the IFT significantly aids oil detachment by lowering capillary forces, which enhances microscopic displacement. A lower IFT helps mobilize residual oil, ultimately improving overall recovery.[6,83,94] Enhanced emulsification further assists oil removal by forming stable oil-in-water emulsions that limit the redeposition of crude-oil components on carbonate surfaces. Together, these mechanisms promote a shift from intermediate oil-wet behaviour to a more water-wet state, ultimately improving microscopic displacement efficiency and enhancing oil recovery in carbonate reservoirs.[43,82,95]

4. Conclusion

The adsorption behaviour of Gemini surfactants (Triamine, Tetramine, Pentamine, and Hexamine GS) derived from mustard oil was comprehensively assessed on sandstone and carbonate rocks under static and dynamic conditions. XRD, XRF, FESEM, and wettability tests were carried out to evaluate the adsorption behaviour of the Gemini surfactants. The key conclusions are:

- The adsorption depends on the spacer length, such as the adsorption of Hexamine GS was consistently reduced as the spacer length increased, with the lowest retention values (0.072 mg g^{-1} in sandstone and 0.057 mg g^{-1} in carbonate after 24 hours).
- Static isotherm analysis indicated that the Langmuir and Redlich–Peterson models provided the optimal fit, confirming monolayer adsorption with heterogeneous contributions. Although Hexamine GS consistently exhibited the lowest q_0 values, which are advantageous for EOR.

© 2026 The Author(s). Published by the Royal Society of Chemistry

Open Access Article. Published on 18 February 2026. Downloaded on 6/19/2026 8:10:42 PM. This article is licensed under a Creative Commons Attribution-NonCommercial 3.0 Unported Licence.

• Kinetic analysis revealed that pseudo-first-order models most accurately represented the data, suggesting that adsorption is primarily governed by physisorption, as evidenced by multi-step diffusion behaviour.

• Thermodynamic characteristics indicate that adsorption was spontaneous and physically driven.

• Dynamic adsorption tests revealed early breakthrough, swift equilibration, and minimal retention for Hexamine GS (0.013 mg g^{-1} for sandstone and 0.008 mg g^{-1} for carbonate) with rapid breakthrough and fast equilibrium. The desorption process was primarily reversible, particularly in carbonate samples, supporting the presence of mild physical interactions.

• Analysis of surface characterization (FESEM-EDX and zeta potential) confirmed the formation of thin surfactant layers, a reduction in surface charge, and unambiguous evidence of surfactant adsorption. The effects were more pronounced in sandstone.

• Contact angle experiments demonstrated that Hexamine GS shows effective reversal of wettability from oil-wet to water-wet, with a reduction of up to 85% within 12 minutes in sandstone and 83% within 15 minutes in carbonate. This confirms the strong potential for improved displacement efficiency.

Thus, Mustard oil-derived Gemini surfactants represent potentially eco-friendly, cost-effective enhanced oil recovery agents, with Hexamine GS showing the greatest promise for use in sandstone and carbonate reservoirs.

Author contributions

Lavisha Jangid: investigation, experimental synthesis and work, formal analysis, data curation, writing the original draft. Keka Ojha: validation, supervision, review & editing. Ajay Mandal: project administration, funding acquisition, data interpretation, review & editing.

Conflicts of interest

The authors declare no competing financial interests or personal relationships that could have influenced the work reported in this paper.

Data availability

All data supporting the findings of this study are provided in the supporting information (SI). Additional raw data can be provided by the corresponding author upon reasonable request. Supplementary information (SI): XRD/XRF mineralogical characterization of the reservoir rocks, adsorption isotherm and kinetic model equations, FESEM–EDX surface analysis data with and without Gemini surfactant treatment, and extended adsorption data under prolonged equilibration conditions. See DOI: https://doi.org/10.1039/d6ra00648e.

Acknowledgements

We extend our sincere appreciation to SPARC, Ministry of Human Resource Development (SPARC/2019-2020/P1672/SL), Syntron Industries Private Limited (No-SYN/2024-25/01) for their generous financial support to the Department of Petroleum Engineering, Indian Institute of Technology (ISM), Dhanbad, India.

References

1 T. Austad, B. Matre, J. Milter, A. Sævareid and L. Øyno, *Colloids Surf., A*, 1998, 117–129.
2 *Improved Oil Recovery by Surfactant and Polymer Flooding*, ed. D. O. Shah and R. S. Schechter, American Institute of Chemical Engineers, Academic Press, New York, 1977.
3 M. S. Kamal, I. A. Hussein and A. S. Sultan, *Energy Fuels*, 2017, **31**, 7701–7720.
4 Y. Yao, M. Wei and W. Kang, *Adv. Colloid Interface Sci.*, 2021, **294**, 102477.
5 Y. Bai, Z. Wang, X. Shang, C. Dong, X. Zhao and P. Liu, *Energy Fuels*, 2017, **31**, 5860–5869.
6 M. Amirpour, S. R. Shadizadeh, H. Esfandyari and S. Ahmadi, *Petroleum*, 2015, **1**, 289–299.
7 H. Guo, K. Song and R. Hilfer, *SPE Improved Oil Recovery Conference*, SPE, 2020, p. D031S046R001.
8 K. Hazarika, S. B. Gogoi and A. Kumar, *Pet. res.*, 2023, **8**, 54–62.
9 J. Salager, A. M. Forgiarini and J. Bullón, *J. Surfactants Deterg.*, 2013, **16**, 449–472.
10 A. F. Belhaj, K. A. Elraies, S. M. Mahmood, N. N. Zulkifli, S. Akbari and O. S. Hussien, *J. Pet. Explor. Prod. Technol.*, 2020, **10**, 125–137.
11 R. Phukan, R. Saha and P. Mazumdar, *J. Surfactants Deterg.*, 2024, **27**, 393–408.
12 M. A. Ahmadi and S. R. Shadizadeh, *Fuel*, 2015, **159**, 15–26.
13 S. E. I. Lebouachera, O. Balamane-Zizi, A. Boublia, M. A. Ghriga, M. Hasanzadeh, H. E. Hadri, D. Tassalit, M. Khodja, B. Grassl and N. Drouiche, *Chem. Afr.*, 2024, **7**, 2283–2306.
14 S. Pal, M. Mushtaq, F. Banat and A. M. Al Sumaiti, *Pet. Sci.*, 2018, **15**, 77–102.
15 P. Somasundaran and L. Zhang, *J. Petrol. Sci. Eng.*, 2006, **52**, 198–212.
16 Z. Chang, X. Chen and Y. Peng, *Miner. Eng.*, 2018, **121**, 66–76.
17 S. E. I. Lebouachera, A. Boublia, M. E. M. Hadji, M. A. Ghriga, D. Tassalit, M. Khodja, B. Grassl and N. Drouiche, *Chem. Pap.*, 2025, **79**, 655–666.
18 M. Hu, L. Liu, N. Hou, X. Li, D. Zeng and H. Tan, *Chemosphere*, 2021, **274**, 129655.
19 S. Liu, Y. Peng, J. Chen, T. Yan, Y. Zhang, J. Liu and J. Li, *J. Hazard. Mater.*, 2020, **382**, 121103.
20 M. Raposo and O. N. Oliveira Jr, *Braz. J. Phys.*, 1998, **28**(4), 392–404.
21 I. Khurshid, E. W. Al-Shalabi and I. Afgan, *SPE Reservoir Eval. Eng.*, 2022, **25**, 397–413.
22 F. L. Leite, C. C. Bueno, A. L. Da Róz, E. C. Ziemath and O. N. Oliveira, *Int. J. Mol. Sci.*, 2012, **13**, 12773–12856.
23 H. V. Helmholtz, Studien über electrische Grenzschichten, *Ann. Phys.*, 1879, **243**(7), 337–382.

© 2026 The Author(s). Published by the Royal Society of Chemistry

Open Access Article. Published on 18 February 2026. Downloaded on 6/19/2026 8:10:42 PM. This article is licensed under a Creative Commons Attribution-NonCommercial 3.0 Unported Licence.

24 O. Stern, *Z. Elektrochem. Angew. Phys. Chem.*, 1924, **30**, 508–516.
25 P. Somasundaran and S. Krishnakumar, *Colloids Surf., A*, 1997, **123–124**, 491–513.
26 J. J. Hamon, R. F. Tabor, A. Striolo and B. P. Grady, *Langmuir*, 2018, **34**, 7223–7239.
27 M. M. Mabrouk, N. A. Hamed and F. R. Mansour, *Appl. Spectrosc. Rev.*, 2023, **58**, 206–234.
28 Y. Wang, H. Xu, W. Yu, B. Bai, X. Song and J. Zhang, *Pet. Sci.*, 2011, **8**, 463–476.
29 S. Chowdhury, S. Shrivastava, A. Kakati and J. S. Sangwai, *Ind. Eng. Chem. Res.*, 2022, **61**, 21–64.
30 M. Amirmoshiri, L. Zhang, M. C. Puerto, R. D. Tewari, R. Z. B. K. Bahrim, R. Farajzadeh, G. J. Hirasaki and S. L. Biswal, *Langmuir*, 2020, **36**, 10725–10738.
31 M. Karimi, R. S. Al-Maamari, S. Ayatollahi and N. Mehranbod, *J. Petrol. Sci. Eng.*, 2016, **147**, 560–569.
32 J. B. Lawson, in *SPE Symposium on Improved Methods of Oil Recovery*, SPE, Tulsa, Oklahoma, 1978, p. SPE-7052-MS.
33 C. Legens, T. Palermo, H. Toulhoat, A. Fafet and P. Koutsoukos, *J. Petrol. Sci. Eng.*, 1998, **20**, 277–282.
34 A. Mamonov, T. Puntervold and S. Strand, in *SPE Russian Petroleum Technology Conference*, SPE, Moscow, Russia, 2017, p. D033S021R003.
35 D. C. Standnes and T. Austad, *J. Petrol. Sci. Eng.*, 2003, **39**, 431–446.
36 P. Somasundaran and L. Huang, *Adv. Colloid Interface Sci.*, 2000, **88**, 179–208.
37 B.-Y. Zhu and T. Gu, *Adv. Colloid Interface Sci.*, 1991, **37**, 1–32.
38 M. Musah, Y. Azeh, J. Mathew, M. Umar, Z. Abdulhamid and A. Muhammad, *Caliphate J. Sci. Technol.*, 2022, **4**, 20–26.
39 H. M. F. Freundlich, *J. Phys. Chem.*, 1906, **57**, 1100–1107.
40 I. Langmuir, *J. Am. Chem. Soc.*, 1916, **38**, 2221–2295.
41 M. A. Ahmadi and S. R. Shadizadeh, *Energy Fuels*, 2012, **26**, 4655–4663.
42 M. Muherei and R. Junin, *Mod. Appl. Sci.*, 2009, **3**, p158.
43 A. Dabiri and B. Honarvar, *J. Surfactants Deterg.*, 2020, **23**, 821–829.
44 N. Pal, N. Saxena and A. Mandal, *Colloids Surf., A*, 2017, **533**, 20–32.
45 Kh. Jarrahian, O. Seiedi, M. Sheykhan, M. V. Sefti and Sh. Ayatollahi, *Colloids Surf., A*, 2012, **410**, 1–10.
46 L. Jangid, S. Dey, D. Joshi, N. Saxena, K. Ojha and A. Mandal, *J. Mol. Liq.*, 2024, **408**, 125326.
47 S. Kumar and A. Mandal, *Appl. Surf. Sci.*, 2016, **372**, 42–51.
48 U. Patel, P. Parekh, N. V. Sastry, V. K. Aswal and P. Bahadur, *J. Mol. Liq.*, 2017, **225**, 888–896.
49 A. Yarahmadi, G. Zargar, S. Ashoori and A. Khaksar Manshad, *Sci. Rep.*, 2026, **16**, 4404.
50 L. Jangid, K. Ojha and A. Mandal, *J. Taiwan Inst. Chem. Eng.*, 2026, **179**, 106462.
51 E. D. Revellame, D. L. Fortela, W. Sharp, R. Hernandez and M. E. Zappi, *Clean Eng. Technol.*, 2020, **1**, 100032.
52 W. J. Weber and J. C. Morris, *J. Sanit. Eng. Div.*, 1963, **89**, 31–59.
53 T. Chen, T. Da and Y. Ma, *J. Mol. Liq.*, 2021, **322**, 114980.
54 A. Barati-Harooni, A. Najafi-Marghmaleki, S. M. Hosseini and S. Moradi, *J. Energy Resour. Technol.*, 2017, **139**, 042202.
55 C. Dai, K. Wang, Y. Liu, H. Li, Z. Wei and M. Zhao, *Energy Fuels*, 2015, **29**, 2304–2311.
56 W. Kwok, R. E. Hayes and H. A. Nasr-El-Din, *Chem. Eng. Sci.*, 1995, **50**, 769–783.
57 J. Eastoe, A. Rankin, R. Wat and C. D. Bain, *Int. Rev. Phys. Chem.*, 2001, **20**, 357–386.
58 D. T. Grow and J. A. Shaeiwitz, *J. Colloid Interface Sci.*, 1982, **86**(1), 239–253.
59 W. Kwok, R. E. Hayes and H. A. Nasr-El-Din, *Chem. Eng. Sci.*, 1995, **50**, 769–783.
60 A. Barati-Harooni, A. Najafi-Marghmaleki, S. M. Hosseini and S. Moradi, *J. Energy Resour. Technol.*, 2017, **139**(4), 042202.
61 H. Naidu and A. Mathews, *Sep. Purif. Technol.*, 2021, **257**, 117955.
62 N. Saxena, S. Kumar and A. Mandal, *Asia-Pac. J. Chem. Eng.*, 2018, **13**, e2211.
63 S. Kalam, S. A. Abu-Khamsin, M. S. Kamal, S. M. S. Hussain, K. Norrman, M. Mahmoud and S. Patil, *Energy Fuels*, 2022, **36**, 5737–5748.
64 M. S. Kamal, S. M. S. Hussain, L. T. Fogang and A. S. Sultan, *Tenside Surfactants Deterg.*, 2018, **55**, 491–497.
65 V. F. Dos Santos Borges, M. K. S. Monteiro, E. D. Da Silva Filho, D. C. Da Silva, J. L. Cardozo Fonseca, A. O. Wanderley Neto and T. Pinheiro Braga, *Langmuir*, 2024, **40**, 19430–19440.
66 S. Kalam, S. A. Abu-Khamsin, M. S. Kamal and S. Patil, *ACS Omega*, 2021, **6**, 32342–32348.
67 M. A. Ahmadi, S. Zendehboudi, A. Shafiei and L. James, *Ind. Eng. Chem. Res.*, 2012, **51**, 9894–9905.
68 Y.-J. Shen, Y.-L. Zhang, F. Gao, G.-S. Yang and X.-P. Lai, *Energies*, 2018, **11**, 1753.
69 N. A. Akabar and M. N. Adlan, *Lect. Notes Civ. Eng.*, 2020, 621–627, DOI: 10.1007/978-3-030-32816-0_43.
70 A. E.-H. A. El- Badry, M. F. Ali and B. M. Ismail, *Sci. Cult.*, 2019, **5**(2), 37–48.
71 M. U. Shafiq, H. K. Ben Mahmud and M. Ghasemi, *Petroleum*, 2019, **5**, 67–76.
72 J. E. Welton, *American Association of Petroleum Geologists (AAPG)*, 1984, pp. 154–175.
73 A. M. Neves, V. C. Santanna, J. L. M. Barillas, T. N. C. Dantas, K. C. Oliveira and A. G. B. Góis, *An. Acad. Bras. Cienc.*, 2021, **93**, e20190534.
74 M. H. Derkani, A. J. Fletcher, M. Fedorov, W. Abdallah, B. Sauerer, J. Anderson and Z. J. Zhang, *Colloids Interfaces*, 2019, **3**, 62.
75 A. Barati, A. Najafi, A. Daryasafar, P. Nadali and H. Moslehi, *Chem. Eng. Res. Des.*, 2016, **105**, 55–63.
76 S. Kalam, S. A. Abu-Khamsin, S. Patil, M. Mahmoud, M. S. Kamal, M. Murtaza and K. K. Mohanty, *Fuel*, 2023, **345**, 128166.
77 S. Khan, A. Gbadamosi, K. Norrman, X. Zhou, S. M. S. Hussain, S. Patil and M. S. Kamal, *Materials*, 2022, **15**, 2527.
78 K. Y. Foo and B. H. Hameed, *Chem. Eng. J.*, 2010, **156**, 2–10.

© 2026 The Author(s). Published by the Royal Society of Chemistry

Open Access Article. Published on 18 February 2026. Downloaded on 6/19/2026 8:10:42 PM.
This article is licensed under a Creative Commons Attribution-NonCommercial 3.0 Unported Licence.

79 A. Isah, M. Arif, A. Hassan, M. Mahmoud and S. Iglauer, *Energy Rep.*, 2022, **8**, 6355–6395.
80 S. Kalam, S. A. Abu-Khamsin, A. O. Gbadamosi, S. Patil, M. S. Kamal, S. M. S. Hussain, D. Al-Shehri, E. W. Al-Shalabi and K. K. Mohanty, *Sci. Rep.*, 2023, **13**, 1–11.
81 L. K. Koopal, W. H. van Riemsdijk, J. C. M. de Wit and M. F. Benedetti, *J. Colloid Interface Sci.*, 1994, 51–60.
82 S. Das, Q. Nguyen, P. D. Patil, W. Yu and R. T. Bonnecaze, *Langmuir*, 2018, **34**, 10650–10658.
83 S. Kumar and A. Mandal, *Appl. Surf. Sci.*, 2016, **372**, 42–51.
84 H. Xu, Y. Li, F. Zhou, H. Su, E. Yao, J. Hu and Z. Chen, *Chem. Eng. J.*, 2023, **470**, 144070.
85 S. LAGERGREN, *K. Sven. Vetenskapsakad. Handl.*, 1898, **24**, 1–39.
86 H. Wang, A. Zhou, F. Peng, H. Yu and J. Yang, *J. Colloid Interface Sci.*, 2007, **316**, 277–283.
87 N. Saxena, A. Kumar and A. Mandal, *J. Petrol. Sci. Eng.*, 2019, **173**, 1264–1283.
88 M. Ghiaci, R. J. Kalbasi and A. Abbaspour, *Colloids Surf., A*, 2007, **297**, 105–113.
89 D. Cao, J. Wang, M. Han and A. J. Alshehri, *Petroleum*, 2022, **8**, 414–423.
90 J. Wang, M. Han, A. B. Fuseni and D. Cao, in *SPE Middle East Oil & Gas Show and Conference*, Society of Petroleum Engineers, Manama, Bahrain, 2015.
91 M. Ayoub, M. E. Mohyaldinn, S. M. Mahmood, A. Aqsha, S. R. Jufar, S. Farrukh, F. Inayat and M. R. Shamsuddin, *J. Pet. Explor. Prod. Technol.*, 2019, **10**, 311–318.
92 B. Hou, Y. Wang, X. Cao, J. Zhang, X. Song, M. Ding and W. Chen, *J. Surfactants Deterg.*, 2016, **19**, 315–324.
93 A. Rezaei, A. Khodabakhshi, A. Esmaeili and M. Razavifar, *Petroleum*, 2022, **8**, 499–508.
94 X. Deng, Z. Tariq, M. Murtaza, S. Patil, M. Mahmoud and M. shahzad Kamal, *J. Mol. Liq.*, 2020, **325**, 115175.
95 S. Ahmadi, M. Hosseini, E. Tangestani, S. E. Mousavi and M. Niazi, *Pet. Sci.*, 2020, **17**, 712–721.

© 2026 The Author(s). Published by the Royal Society of Chemistry